Meteoritics & Planetary Science 40, Nr 8, 1215–1239 (2005)
Abstract available online at http://meteoritics.org

Weathering of meteorites from Oman: Correlation of chemical and mineralogical weathering proxies with ^{14}C terrestrial ages and the influence of soil chemistry

A. AL-KATHIRI[1, 2*], B. A. HOFMANN[3], A. J. T. JULL[4], and E. GNOS[1]

[1]Institut für Geologie, Universität Bern, Baltzerstrasse 1, CH-3012 Bern, Switzerland
[2]Directorate General of Commerce and Industry, Ministry of Commerce and Industry, Salalah, Oman
[3]Naturhistorisches Museum der Burgergemeinde Bern, Bernastrasse 15, CH-3005 Bern, Switzerland
[4]National Science Foundation Arizona Accelerator Mass Spectrometry Laboratory,
University of Arizona, 1118 East Fourth Street, Tucson, Arizona 85721, USA
*Corresponding author. E-mail: alikath@geo.unibe.ch

(Received 05 January 2005; revision accepted 15 July 2005)

Abstract–Fifty-four fragments of ordinary chondrites from 50 finds representing all searched areas in central Oman and all weathering stages were selected to compare the physical, chemical, and mineralogical effect of terrestrial weathering with ^{14}C terrestrial ages. ^{14}C ages range from 2.0 to >49 kyr with a median value of 17.9 kyr. The peak of the age range, which is between 10–20 kyr, falls in an arid climate period. A comparison of the chemical composition of Omani chondrites with literature data for unweathered H and L chondrites demonstrates a strong enrichment in Sr and Ba, and depletion in S during weathering. Water contents in H chondrites increase with terrestrial age, whereas L chondrites show a rapid initial increase followed by nearly constant water content. Correlating Sr, Ba, and H_2O with age indicates two absorption trends: i) an initial alteration within the first 20 kyr dominated by H_2O uptake, mainly reflecting Fe-Ni metal alteration, and ii) a second Ba- and Sr-dominated stage correlated with slower and less systematic weathering of troilite that starts after H_2O reaches ~2 wt%. Sulfur released from troilite partly combines with Ba and Sr to form sulfate minerals. Other parameters correlated with ^{14}C age are degree of weathering, color of powdered meteorites, and the Ni/Fe ratio. Chemical analyses of 145 soils show a high degree of homogeneity over the entire interior Oman Desert, indicating large-scale mixing by wind. Soil samples collected from beneath meteorite finds typically are enriched in Ni and Co, confirming mobilization from the meteorites. High Cr and Ni concentrations in reference soil samples, which decrease from NE to SW, are due to detrital material from ultramafic rocks of the Oman Mountains.

INTRODUCTION

Since 1999, Oman has become an important country for the recovery of hot desert meteorites (Grossman 2000; Grossman and Zipfel 2001; Russell et al. 2002, 2003, 2004). Before 1999, studies on Omani meteorites were limited to using six museum specimens (Franchi et al. 1995). A joint meteorite search program involving geologists from Bern, Switzerland (University of Bern and Natural History Museum Bern), and the Ministry of Commerce and Industry, Sultanate of Oman, was initiated in 2001. This search has resulted in the recovery of specimens from more than 263 individual falls during three field seasons in 2001–2003 (excluding thousands of samples from some large strewn fields, mainly Jiddat al Harasis [JaH] 073).

When meteorites reach the Earth's surface, they are exposed to a range of potential weathering agents such as water, oxygen-rich air, salts, wind, and temperature variations. Other factors, including the composition and porosity of meteorites and host soils/bedrocks, may also influence the mechanisms and rates of weathering. Weathering rates will further depend on the climate history since the fall occurred. As the degree of weathering of meteorites increases with their terrestrial age, old surfaces are likely to yield more highly-weathered meteorites than younger surfaces. Due to meteorite accumulation over long periods of time, hot or cold desert environments are most suitable for weathering studies (Bischoff and Geiger 1995; Bland et al. 1996; Stelzner et al. 1999; Welten 1999; Lee and Bland 2004).

In this paper, we investigate weathering-induced mineralogical and chemical changes of meteorites recovered from various areas in the central Oman Desert, compare weathering-related parameters (fragmentation, dispersion of fragments on the soil, alteration mineralogy, color of powdered meteorites, bulk chemistry) with ^{14}C terrestrial ages, and put these findings into the context of the geological and climatic history. The meteorites used for this study were described in the Meteoritical Bulletins 87–88 (Russell et al. 2003, 2004).

It is important to note that the regions as defined by the Meteoritical Society's Nomenclature Committee (Fig. 1) do not overlap fully with the geographical use of the names. Dhofar (Dho) and Jiddat al Harasis, for example, are geographical areas much larger than the area where meteorites are named Dho or JaH. Except in direct connection with meteorite names, our use of such names refers to the geographical usage.

GEOLOGY OF THE INTERIOR OMAN DESERT

The central plains of the interior of Oman comprise more than 50% of the area of the country (Le Métour et al. 1995). These essentially flat areas lie at an altitude of between 50 and 250 m and are underlain by limestone, predominantly Miocene in age (minor Oligocene and Eocene). The horizontal bedding has remained largely undisturbed since marine deposition, with the exception of local salt tectonics. The area forms a vast peneplain partially covered by a layer of rocky debris. The Jiddat al Harasis is the largest of these limestone plains. It crops out extensively around Hayma and has almost no drainage network. These limestone plains are partially covered by aeolian sand dunes, which are still being shaped by the desert winds. These dune fields constitute the immense Rub al Khali Desert, and dunes accumulate locally to form ramlats (dune fields) in the north of Dhofar. A vast inland depression is located to the northeast of the central plains, the Umm as Samim sabkhah. Vast alluvial fans form a transitional belt to the Oman Mountains. Bedrock in the meteorite search area in the central Oman Desert consists mainly of the Hadhramaut Group (Bydoun 1966) and the Fars Group (Hughes-Clarke 1988). Both groups can be divided into marine and continental units (Chevrel et al. 1992). The Hadramaut marine deposits include highly recrystallized, nodular to thinly-bedded gray to brown limestone or dolostone (Platel et al. 1992) whereas the lacustrine deposits consist of micritic chalky limestone (Platel and Berthiaux 1992a, 1992b). The Fars marine deposits include green marl grading upwards into massive bioclastic and brecciated limestone (Platel and Berthiaux 1992b). The continental units includes gray to white micritic and brecciated lacustrine limestone, reddish conglomerate, and reddish siltstone and clay (Platel and Berthiaux 1992a). To the north, these rocks grade into a purplish red brecciated limestone (Chevrel et al. 1992). Quaternary deposits of the region are mainly wadi (a dry river occasionally flooded after heavy rain showers) sands and aeolian sand deposits consisting of high sand mounts, low active sand dunes, and aeolian sand veneers. Small domains of sub-recent to recent piedmont deposits and ancient to sub-recent travertine deposits crop out locally.

CHARACTERIZATION OF METEORITE COLLECTION SURFACES AND CLIMATIC CONDITIONS

The Omani meteorite recovery areas are mainly restricted to the flat carbonate plains, where erosion and deposition since Tertiary deposition have been limited and meteorites have had a chance to accumulate over prolonged periods of time. The color/brightness contrast between the dark meteorites and the light carbonate surfaces facilitates identification of the meteorites.

Several areas of high meteorite find density occur in the Oman Desert. Find density is mainly a result of search intensity and suitability for search. The main collection areas are shown in Fig. 1. Collection surfaces typically consist of totally flat, loose limestone desert pavements, with silt/sand-sized fine material between limestone rocks. The average size of rock particles varies from a few mm to about 10 cm. Areas subject to slight erosion, with slightly irregular surface and larger limestone fragments (up to several cm), can be distinguished from obviously older peneplains, showing a reddish coloration of the surface and exhibiting smaller (typically 1 cm) limestone fragments. Shallow pits and rare sections exposed along wadis and road cuts show that soil formation can reach several meters deep at places, while in other areas limestone bedrock is exposed at the surface. Evidence for ponding of water after rare showers is common in shallow depressions (khabras) in the form of local sandy or clayey sediments displaying desiccation cracks. The climate in the searched area is dry and hot, with annual mean precipitation below 100 mm, in the Rub al Khali area below 50 mm (Sanlaville 1992). Yalooni station (18°56′N, 57°06′E) reports a mean annual rainfall 1981–1991 of 43.4 mm (annual variations 0–230 mm). Precipitation is mainly from cyclonic storms. However, the Indian Ocean is 35 to 230 km from collection areas and humid air is additionally brought into the desert by moist coastal air with common morning fog. Temperatures reach 50 °C in summer and can go below 0 °C occasionally during winter nights. We recorded January/February temperatures of 20–31 °C during the day and 4–12 °C during nights, and relative humidity of 30% to >90%. The dew point is frequently reached during winter in early morning hours, resulting in a wetting of rock, soil, and meteorite surfaces. Vegetation is sparse. Towards the coast, acacia trees are more common and rocks show a frequent cover by lichen, indicating higher availability of humidity.

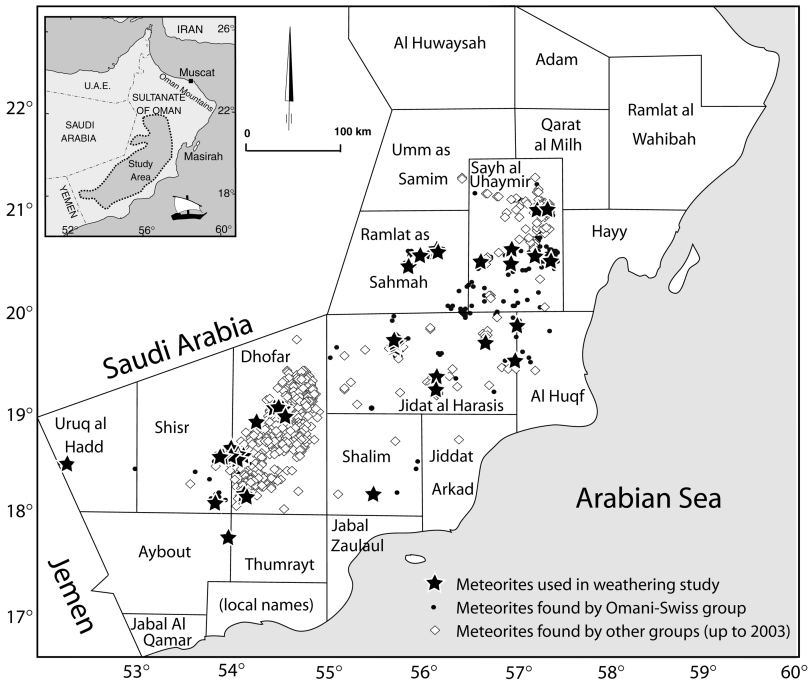

Fig. 1. Distribution of meteorite finds in Oman. Stars mark meteorites used in this study. Filled circles are meteorites collected during the Omani-Swiss meteorite search project until 2003. Diamonds represent published finds by other groups until 2003. Name boundaries are from the Meteoritical Society.

The present-day climate is representative of the last ~6 kyr, but older meteorites may have been subjected to several periods of wetter conditions (Sanlaville 1992; Burns et al. 2000; Fleitmann et al. 2003, 2004).

SAMPLES AND METHODS

From the total of ~263 ordinary chondrite finds during our search program, 54 meteorite fragments from 50 individual finds representing as large a spread of weathering as possible were selected for chemical analysis and ^{14}C dating (Fig. 1). In the suite of dated samples, most chondrites with a low degree of weathering (W1) were intentionally included. Additionally, a sample of the Ghubara L5 chondrite was purchased and included in the set of samples, because this is one of the least weathered meteorites from Oman with a ^{14}C terrestrial age of 2–3 kyr (Ferko et al. 2002).

In addition to the meteorites, two types of soil samples were collected: i) 97 samples of soil under meteorites (SUM), and ii) 48 reference soil samples (RSS), typically taken from the top 5 cm of the soil at a distance of about 10 m from meteorite finds (including two calcrete samples from a depth of 20 cm). SUM samples were collected from beneath meteorites that were sufficiently large (>200 g) and firmly embedded in the soil. In strewn fields comprising several to hundreds of meteorite fragments, only a few representative soil samples were collected. RSS were collected from all major collection areas to represent all the different lithological formations. Soil samples typically consist of two major components: i) fine-grained silty material and ii) fragments of the bedrock up to several cm in size.

The mineralogy, including the weathering grades based on the Wlotzka (1993) scale, of all recovered meteorites and a few samples from each strewn field was studied in polished thin sections using transmitted and reflected light microscopy. For classification of meteorites, mineral chemistries of olivine and pyroxene were determined at the University of Bern, Bern, Switzerland, with a Cameca SX-50 microprobe equipped with wavelength dispersive spectrometers using natural and synthetic mineral standards, and beam conditions of 15 kV and 20 nA for silicates. The mineralogy of alteration phases was determined by reflected light microscopy using oil immersion, allowing the discrimination of magnetite, hematite, maghemite, and Fe-hydroxides. XRD was applied for the detection of specific minerals using powder sedimented on a silicon wafer and a Philips PW1800 diffractometer. Semi-quantitative mineral compositions for identification of alteration phases were obtained using energy dispersive X-ray spectrometry (EDS) on a SEM (CamScan CS4).

Cosmogenic ^{14}C was extracted from 200 to 850 mg (typically ~500 mg) meteorite samples using methods described previously (Jull et al. 1989, 1990, 1993, 1998) and measured by accelerator mass spectrometry (AMS) at the University of Arizona, Tucson, Arizona. For bulk chemistry, 47 fragments from 39 meteorites (Table 1) were ground in an agate mill and 5 g of each sample were submitted to Activation Laboratories (Ancaster, Ontario, Canada) for

Table 1. Weathering parameters compared with the ^{14}C-terrestrial age for 39 ordinary chondrites.

Meteorite	Type	Age (kyr)	Error (1σ) (kyr)	Alteration (W)	Fragmentation index (FI)	No. of fragments	Fragment dispersion (FD) (cm)	Meteorite powder color	Meteorite powder color (class)
Mean H chondrites	H								
Aybut 001	H6	5.1	1.3	1–2	1	1	0	5 YR 4/4	4
UaH 002	H3	9.4	1.3	1	1	1	0	5 YR 6/4	6
SaU 228	H6	9.7	1.3	2	1	1	0	5 YR 2/2	2
Dho 1005	H3/4	12.6	1.3	4	1	1	0	10 R 5/4	7
Dho 020	H4/5	12.7	1.3	4	1	1	0	10 R 5/4	7
Shalim 003	H5	13.0	1.3	3	0.51	50	250	10 YR 2/2	2
Dho 814	H5	14.1	1.3	2	1	1	0	5 YR 4/4	4
Dho 1010	H4	14.7	1.3	3	1	1	0	5 YR 3/2	3
SaU 219	H4	15.3	1.3	3	1	1	0	5 YR 2/2	2
Dho 794	H6	16.1	1.3	4	1	1	0	5 YR 2/2	2
Dho 819	H4	16.2	1.3	3	1	1	0	5 YR 2/2	2
Dho 802	H6	17.8	1.4	2	1	1	0	5 YR 6/4	6
Dho 787 L*	H4	19.6	1.3	4	0.16	17	2000	5 YR 6/4	6
Dho 835	H5	26.8	1.4	4	1	1	0	10 R 5/4	7
SaU 259	H4	27.2	1.4	4	0.73	17	300	5 YR 6/4	6
JaH 069 L*	H5	34	1.8	4	0.89	10	560	10 R 5/4	7
Shişr 020	H<4	36.5	2.6	3	0.98	4	720	10 R 5/4	7
JaH 102	H4	41.4	3.9	4	0.16	67	2000	5 YR 6/4	6
Dho 807	H5	>47		2	1	1	0	5 YR 3/2	3
SaU 163 L*	H5	>49		3–4	0.55	36	300	5 YR 6/4	6
Mean <15 kyr				2.6	0.85	8.2	250		5
Mean 15–30 kyr				3.5	0.85	6.3	357		5
Mean >30 kyr				3.1	0.67	27	755		5.5
Mean L chondrites	L								
Ghubara	L5	2–3	1.3	0	1	1	0	N3	1
AH 011*	L6	3.0	1.3	1–2	0.79	101	156	5 YR 4/4	4
SaU 001	L4,5	5.5	1.3	1	1.00	1	130	5 YR 4/4	4
Dho 1012	L6	10.8	1.3	1	1	1	0	5 YR 3/2	3
RaS 113	L6	13.1	1.3	3	1	1	0	5 YR 3/2	3
Shişr 025	L6	13.2	1.3	2	0.97	8	0	5 YR 5/6	5
RaS 111	L6	15.8	1.3	2	0.88	2	4	5 YR 4/4	4
JaH 073 (av 4)**	L6	19.7	1.3	2–4	0.92	2768	0		4
JaH 091	L5	19.3	1.3	3	0.04	1000	5000	5 YR 3/2	3
SaU 235	L6	22.5	1.3	4	0.32	80	300	5 YR 6/4	6
RaS 110	L6	23.3	1.3	4	0.13	50	100	10 R 5/4	7
Dho 805	L6	30	1.6	3–4	1	1	0	10 R 5/4	7
SaU 165	L5	31.1	1.5	4	0.41	3	200	5 YR 6/4	6
SaU 194	L6	34.0	1.6	4	1	1	0	10 R 5/4	7
Shişr 015	L5	36.5	2.4	4	0.53	20	125	5 YR 6/4	6

Table 1. *Continued.* Weathering parameters compared with the ^{14}C-terrestrial age for 39 ordinary chondrites.

Meteorite	Type	Age (kyr)	Error (1σ) (kyr)	Alteration (W)	Fragmentation index (FI)	No. of fragments	Fragment dispersion (FD) (cm)	Meteorite powder color	Meteorite powder color (class)
RaS 112	L6	38.2	2.4	4	0.86	4	200	10 R 5/4	7
Dho 806	L5	41.2	4.3	4	1	1	0	10 R 5/4	7
Dho 005 L*	L6	>47		4	0.56	>100	370	5 YR 6/4	6
Dho 813	L5	>49		3	1	1	0	5 YR 6/4	6
Mean <15 kyr				1.5	0.96	18.8	47.7		3
Mean 15–30 kyr				3	0.55	650	901		5
Mean >30 kyr				4	0.77	>5	128		6

Table 1. *Continued.* Weathering parameters compared with the ^{14}C-terrestrial age for 39 ordinary chondrites.

Meteorite	Iron oxide (vol%)	Troilite oxide (vol%)	Max. oxide veins (μm)	Ba (ppm)	Sr (ppm)	Li (ppm)	S (wt%)	Fe (wt%)	Co (ppm)	Ni (ppm)	Zn (ppm)	As (ppm)	Ir (ppm)	H_2O (wt%)
Mean H chondrites				3.5	9.5	1.7	2.2	27.6	834	16850	51	2	0.77	
Aybut 001	25	5	8	4.7	20	1.3	1.1	29.6	808	14600	73	4.8	0.57	1.78
UaH 002	15	0	15	8	61	1.3	1.5	28.7	846	15600	78	3.8	0.53	2.04
SaU 228	50	5	15	6.2	13	2	1.2	25.3	800	15000	83	2*	0.56	0.72
Dho 1005	100	90	120	53	216	1.7	0.6	26.3	590	12000	89	2.1	0.57	2.44
Dho 020	95	80	180	72	291	2.6	0.4	25.9	608	11900	73	1.8	0.56	2.6
Shalim 003	95	20	300	5.1	19	1.1	1.6	24.1	780	14500	76	2.8	0.46	2.01
Dho 814	40	2	10	11	80	1.5	1.5	29.1	849	16600	66	2.7	0.58	1.8
Dho 1010	95	30	25	4	42	1.6	1.4	24.1	745	16000	66	2*	0.59	2.12
SaU 219	100	40	12	6.1	108	3.9	1.4	23.1	728	14800	84	1.3	0.54	2.12
Dho 794	100	90	70	12	82	1.1	1.4	26.4	780	14000	81	3.7	0.54	2.08
Dho 819	99	20	50	26	108	1.8	1.5	26.1	744	14300	87	1.8	0.51	2.66
Dho 802	60	1	50	18	133	2.3	1.3	26.4	702	13900	76	2.2	0.56	2.41
Dho 787 L*	100	60	100	35	173	2	0.4	25.8	452	7520	71	2.8	0.41	2.22
Dho 835	100	99	10	122	895	2.1	0.7	27	662	12300	59	3.4	0.53	2.35
SaU 259	100	99	75	26	209	2.8	0.3	21.8	533	10800	62	1.3	0.53	2.78
JaH 069 L*	95	5	120	150	594	2.1	0.4	30.3	750	13200	75	4.6	0.63	2.62
Shişr 020	99	40	30	265	938	2.2	0.5	29.6	733	13200	79	3.9	0.62	2.83
JaH 102	99	95	150	95	399	2.1	0.6	24.8	740	14500	69	1.9	0.55	3.37
Dho 807	60	5	100	5.8	28.45	1	0.8	30.3	883	17600	125	1.4	0.59	1.03
SaU 163 L*	98	10	400	101	228	4	0.6	28.5	745	14100	69	0.5	0.67	3.32
Mean <15 kyr	68	29	104	22	102	1.6	1.1	26.5	720	13747	75	3	0.54	1.97
Mean 15–30 kyr	94	52	61	49	288	2.2	0.9	25.9	669	12603	74	2.6	0.53	2.41
Mean >30 kyr	89	38	160	117	398	2.3	0.6	28.3	775	14850	85	1.9	0.61	2.64
Mean L chondrites				3.5	11	1.8	2.2	21.8	550	11530	58	1.5	0.4	
Ghubara	1	0	20	4.5	11	1.2	0.6	25	599	12100	84	1.5*	0.37	0.10
AH 011*	70	10	20	9.1	64	2.8	1.4	23	549	10205	79	2.5	0.37	2.15
SaU 001	70	10	20	5.2	25	1.4	1.7	25.3	584	12100	85	1.5*	0.45	1.45
Dho 1012	3	1	20	4.6	34	1.6	0.5	22.6	775	15100	81	1.5	0.42	0.46

Table 1. *Continued.* Weathering parameters compared with the ^{14}C-terrestrial age for 39 ordinary chondrites.

Meteorite	Iron oxide (vol%)	Troilite oxide (vol%)	Max. oxide veins (μm)	Ba (ppm)	Sr (ppm)	Li (ppm)	S (wt%)	Fe (wt%)	Co (ppm)	Ni (ppm)	Zn (ppm)	As (ppm)	Ir (ppm)	H_2O (wt%)
RaS 113	95	10	60	14	33	3.1	1.7	21.8	560	12700	69	1.5*	0.35	1.37
Shişr 025	90	30	20	115	51	1.4	1	21.9	528	10300	84	2.5	0.45	2.56
RaS 111	30	5	30	3.7	17	1.4	1.2	20.5	548	12400	66	1.5*	0.41	1.42
JaH 073 (av 4)**	93	40	49	49	120	3.1	1.4	22.1	450	9753	74	1.8	0.4	2.30
JaH 091	95	40	15	3	13	1.1	0.8	20.4	550	11900	75	1.5*	0.4	2.29
SaU 235	100	95	70	4.3	34	1.9	0.4	17.6	409	7950	77	1.5*	0.34	2.15
RaS 110	100	80	40	13	130	2.8	0.5	21.5	465	9400	69	1.5*	0.4	2.73
Dho 805	95	30	20	16	87	2.2	0.6	24.5	541	9740	91	1.5	0.4	2.25
SaU 165	100	95	50	45	209	1.2	0.2	26.6	571	10700	97	3.3	0.4	2.47
SaU 194	100	95	40	73	181	14	0.8	24	644	13600	87	2.8	0.5	2.56
Shişr 015	100	10	15	12	133	1.5	0.4	22.5	505	9760	217	1.3	0.46	2.51
RaS 112	100	99	80	13	177	1.5	0.3	21	352	7020	62	1.5*	0.43	2.17
Dho 806	100	80	60	39	314	2.1	0.4	26.4	559	10800	120	3.9	0.48	2.17
Dho 005 L*	100	98	65	41	249	2.4	0.3	24.2	388	6917	95	2.5	0.4	2.03
Dho 813	80	20	40	150	1140	2.40	0.8	23.8	601	10000	93	1.9	0.45	2.36
Mean <15 kyr	55	10	27	25	36	1.9	1.2	23.2	599	12084	80	1.8	0.40	1.35
Mean 15–30 kyr	86	48	37	15	67	2.1	0.8	21.1	494	10190	75	1.6	0.39	2.18
Mean >30 kyr	97	71	50	53	343	3.6	0.5	24.1	517	9828	110	2.5	0.45	2.32

2*, 1.5* = Mean H or L chondrite values are used instead of measurements below detection limit.

** = Fragmentation and dispersion of fragments based on 806 individuals.

AH 011* = Mean of the paired meteorites AH 010 and AH 011.

L* = Terrestrial age obtained after leaching the samples with ethanolamine thioglycollate.

(av 4) = Average chemical analysis of four samples from JaH 073.

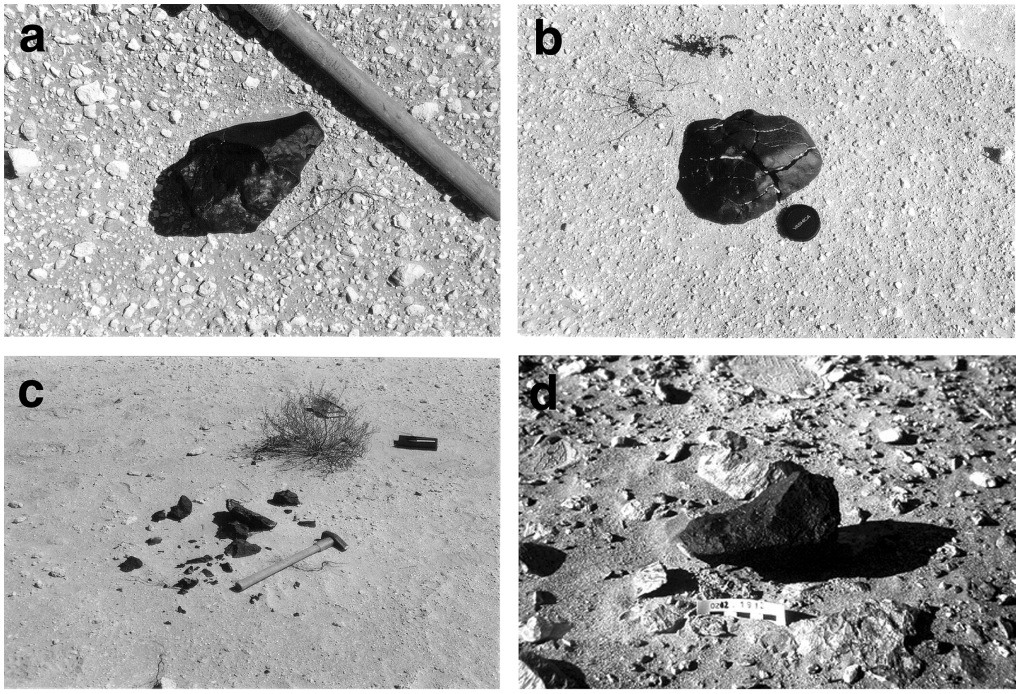

Fig. 2. Weathered meteorites recovered from the Oman Desert: a–c are from the JaH 073 strewn field and illustrate the effect of weathering on meteorites and its possible dependence on the surface type. a) Fresher (W2) meteorite with no weathering fractures on hard soil. b) Weathered (W3) meteorite with cross cutting fractures filled with calcite on softer soil. c) Fragmented, heavily weathered (W4) meteorite in sandy depression; a–c demonstrate the occurrence of different weathering grades within the same strewn field. d) The effect of aeolian abrasion on the meteorite Sayh al Uhaymir (SaU) 259, which is comparable to its effects on surrounding limestone rocks.

detailed analysis using a combination of INAA, ICP-MS, and ICP-OES.

The water content of meteorites was determined gravimetrically on powdered samples using the Penfield method at the Institute for Geological Science, University of Bern. Samples were dried at 105 °C prior to analysis.

Soil samples were sieved to obtain the <0.15 mm fraction, which was used for analyses. Thus, limestone fragments were excluded from the analyses. One hundred and forty-four soils, including two caliche samples, were analyzed without further treatment by ICP-OES following aqua regia extraction (Activation Laboratories). Thirty soil samples, including 1 sample at 20 cm below the surface, were ground in an agate mill and aliquots of 5 g were submitted for more detailed bulk analysis by a combination of INAA, ICP-MS, and ICP-OES.

Heavy minerals were separated from about 40 g of the <0.15 mm soil fraction from 8 RSS. The soils were treated with 5% HCl to remove carbonates and repeatedly washed in a beaker with demineralized water to remove clays. After drying, the heavy mineral fraction was separated using bromoform (density of 2.89 g/cm^3) and the heavy mineral content was determined gravimetrically. Polished thin sections were prepared from the low magnetic fraction of the heavy mineral concentrates and were analyzed on the electron microprobe.

RESULTS

Effects of Weathering Measured in the Field: Fragmentation, Fragment Dispersion, Aeolian Abrasion

We often found meteorites as single, more or less complete individuals. In many other cases, individuals were broken into a number of fragments, typically along cracks formed due to volume expansion during alteration and/or temperature fluctuations (Fig. 2). In extreme cases, fragments were distributed over an area of hundreds of square meters. Only in one case (JaH 091) does this fragmentation appear to be due to impact resulting in a breccia composed of meteorite and bedrock fragments. In all other cases we assume it to be due to physical and chemical weathering (temperature fluctuations and volume increase). In Table 1, we list the fragmentation index (FI) and the fragment dispersion factor (FD). The FI is defined as the mass of the largest fragment/total mass of all fragments as a measure of fragmentation of individuals. The FD is defined as the maximum distance between different fragments of a single fall. For the JaH 073 strewn field, the average FI was calculated from 806 individuals. The reasons for movement of meteorite fragments across the flat-lying soil are unclear. Possible factors are soil creep, water flow after rare heavy rain showers, wind and possibly movement by higher organisms

(birds, antelopes, camels, and man). The largely undisturbed JaH 073 strewn field demonstrates that these processes do not result in a systematic large-scale displacement of meteorites in >10,000 yr.

Rocks and meteorites lying on the surface of a flat desert plain are subject to mechanical erosion by aeolian abrasion, an effect also observed in other desert areas (Schlüter et al. 2002). Desert rocks are more eroded on the sides facing the direction of prevailing wind (Fig. 2d). Aeolian abrasion forms curved features and small slopes, with striations parallel to wind direction, on rock surfaces facing wind directions. Shaped curved surfaces with strong wind striation indicate the main aeolian abrasion direction. We found that rocks (including meteorites) occurring near sand dunes are more abraded. Measuring striations caused by aeolian abrasion shows two main wind directions, a stronger one from the southeast (130–140°) and a weaker one from the north (10°), mainly in the Jiddat al Harasis and Sayh al Uhaymir meteorite areas. Orientations of aeolian striations slowly shift to a dominant north direction (350–010°) towards southern (Shişr) areas, and abrasion intensity becomes weaker.

Aeolian abrasion features are relatively uncommon on the meteorites collected and are probably much less important than chemical weathering, only a few meteorites show aeolian abrasion surfaces similar to those of the surrounding limestones (Fig. 2d).

Terrestrial Ages of Meteorites from Oman

Out of 54 dated ordinary chondrites, 50 contain detectable amounts of ^{14}C, indicating an age of <47,000 yr for the majority of finds (Tables 1 and 2). Only four samples did not contain any detectable ^{14}C. Out of the dated samples, three were from the Dhofar 005 strewn field and three from the JaH 073 strewn field (Table 2). Ages obtained on JaH 073 range from 18.0 to 21.5 ± 1.3 kyr. For the purpose of this study, we use the mean value of 19.7 kyr for JaH 073. After assessment of pairings and including the Ghubara L5 chondrite (Franchi et al. 1995; Ferko et al. 2002), we obtained terrestrial ages from 50 chondrites. Previously dated finds include a CV3 (Sayh al Uhaymir [SaU] 202), 6.8 kyr, the lunar meteorite SaU 169, <9.7 kyr (Gnos et al. 2004); and the shergottite SaU 094, ~12.9 kyr (Gnos et al. 2000). The Ghubara L5 is the youngest meteorite so far reported from Oman. Its almost unaltered composition seems to indicate that maybe it is a recent fall. Its ^{14}C concentration of ~38 dpm/kg indicates a terrestrial age of 2–3 kyr (Ferko et al. 2002), whereas the average $^{14}C/^{10}Be$ ratio of ~2.24 (Ferko et al. 2002) is very close to the average production ratio of ~2.5, suggesting that Ghubara could be younger than 1000 yr. The lunar meteorite Dho 025, dated at 500–600 kyr (Nishiizumi and Caffee 2001), and the shergottite Dho 019, dated at 360 kyr (Nishiizumi et al. 2002), have the longest terrestrial ages for meteorites from Oman.

In order to address the possibility of a contamination of weathered meteorites with terrestrial ^{14}C we leached seven samples with ethanolamine thioglycollate (Table 2), a compound used to selectively dissolve iron oxides and hydroxides (Cornish and Doyle 1984). This approach was based on the assumption that organic contaminations would likely be associated with weathering products. All samples were further treated in the usual way (see Samples and Methods section), including phosphoric acid treatment, to remove carbonates. In three of the leached samples, ^{14}C concentrations were lower by 0.46 to 4.03 dpm/kg after leaching (in two cases reaching values below detection). In four cases, concentrations were increased by 0.89 to 3.87 dpm/kg. These variable data could be due to removal of contaminating ^{14}C, data scatter, contamination during treatment, and/or heterogeneous distribution of ^{14}C.

Meteorite Powder Color and Weathering Grade

Using the rock-color chart (Goddard et al. 1948), the color of meteorite powders prepared for geochemical analysis were compared with weathering grade (Wlotzka 1993) to test if there is any relationship between the intensity of weathering and the color of the powders. Metal and troilite in meteorites are altered to yellowish red iron hydroxides and iron oxides. With increasing weathering grade, the powder colors are increasingly dominated by the color of the weathering products. Powder colors were grouped to seven classes (Table 1). Fresh unweathered meteorites have a dark gray color (N3). With increasing amounts of weathered metal and troilite, the powder commonly grades to dusky brown, grayish brown, moderate brown, and finally light brown (5 YR 6/4) for strongly weathered meteorites (W3, W4). Some strongly weathered meteorites, e.g., Dho 794 (W4), are characterized by an unusually high abundance of magnetite causing unusually dark powders (Table 1), commonly grayish brown (5 YR 2/2).

Mineralogy of Weathering Products

All the meteorites collected, plus a few representative samples from each strewn field, were studied in polished thin sections using transmitted and reflected light microscopy. Microscopically, alteration in silicate minerals is restricted to staining with Fe-hydroxide particles. This is probably similar to the aggregates of goethite formed after smectite as a product of the initial rapid weathering as described by Bland et al. (1998c). In a meteorite powder (SaU 163), small amounts of smectitic clay minerals were detected by XRD after Fe-hydroxide dissolution using ethanolamine thioglycollate and enrichment of the fine-grained fraction of the powder by sedimentation of larger particles. Fe-Ni alloys and sulfide (troilite) are weakly to completely altered, corresponding to weathering grades W1–W4 (Wlotzka 1993). The alteration

Table 2. Terrestrial ages of various Omani meteorites: additional ordinary chondrites that have no chemical analysis, ordinary chondrites leached with ethanolamine thioglycollate, a carbonaceous chondrite, a lunar meteorite, and a Martian meteorite.

Meteorite	Type	Bulk ^{14}C (dpm/kg)	Error (1σ) (dpm/kg)	Leached sample ^{14}C (dpm/kg)	Age (kyr)	Error (1σ) (kyr)	Leached sample age (kyr)
H chondrites							
SaU 209	H5 S1 W2	26.12	0.13		4.8	1.30	
Dho 816	H5 S2 W2	2.95	0.18		6.6	1.30	
Dho 799	H4 S2 W3	13.35	0.28		10.3	1.3	
JaH 120	H5 S1 W2	11.52	0.14		11.5	1.3	
Dho 787	H4 S1/2 W4	4.34	0.13		19.6	1.3	
Shişr 032	H5 S2 W1	10.27	0.13		12.5	1.3	
Ras 114	H5 S1/2 W3	3.81	0.16		20.7	1.3	
SaU 250	H4–6 S2 W3	3.66	0.13		21.0	1.3	
Dho 835	H5 S1/2 W4	1.82	0.13	3.72 ± 0.14	26.8	1.4	20.9 ± 1.3
Shişr 020	H4–6 S1 W3	0.56	0.15	2.70 ± 0.21	36.5	2.6	23.5 ± 1.4
Dho 999	H5 S1 W4	1.07	0.23		31.2	2.2	
JaH 069	L5 S1/2 W4	1.62	0.25	0.83 ± 0.23	28.5	1.8	34 ± 2.6
Shişr 017	H4 S5 W4	0.66	0.14		35.1	2.2	
SaU 163	H5 S1/2 W3–4	3.56	0.15	−0.47 ± 0.20	21.2	1.3	>50
L chondrites							
UaH 001	LL5 S2 W2	12.73	0.16		12.1	1.3	
JaH 078	L6 S4 W2	5.36	0.10		18.7	1.3	
Jah 073	L6 S4 W3	5.76	0.12		18	1.3	
Jah 073	L6 S4 W2	4.75	0.09		19.6	1.3	
Jah 073	L6 S4 W4	3.79	0.11		21.5	1.3	
Dho 005	L6 S4 W4	0.75	0.14		34.6	2	
Dho 005	L6 S5(4) W4	0.56	0.10	4.43 ± 0.20	37.4	2.0	20.2 ± 1.4
Dho 005	L6 S4/5 W4	0.37	0.13	−0.09 ± 0.28	40.6	3.1	>47 ± 26.6
Dho 813	L5 S4 W3	−0.14	0.14	0.75 ± 0.12	>49		34.9 ± 1.9
Various meteorites							
SaU 202	CV3 2/3.3	26.05	0.28		6.8	1.3	
SaU 169[a]	Lunar	20.23	0.26		9.7	1.3	
SaU 094	Martian	12.77	0.26		12.9	1.3	

[a] $^{10}Be = 8.05 \pm 0.30$ dpg/kg.

products occur as replacements of pre-existing minerals and as matrix staining and veins cross-cutting the meteorites. Typically, it is observed that weathering in Fe-Ni proceeds faster than in troilite, in some cases the metal alloy is completely weathered, while troilite shows only minor weathering. Similarly, Lee and Bland (2004) observed almost completely altered Fe-Ni metal besides considerable volumes of troilite, which remained unaltered in hot desert meteorites. We classified several alteration features to provide a refined alteration scheme for ordinary chondrites and to compare these weathering parameters with ^{14}C ages (Table 1).

Fe-Ni metal shows an initial development of oxide/hydroxide coatings leading to total replacement of metal grains in advanced stages of alteration. Boundaries between fresh Fe-Ni and alteration phases are always sharp. Taenite shows a somewhat higher degree of resistance than kamacite and can sometimes be observed as relicts. The alteration mineralogy is dominated by maghemite and Fe hydroxides, but magnetite and hematite are commonly observed as well (Fig. 3a). In a few meteorites, magnetite and hematite are the dominant minerals replacing Fe-Ni, most prominent in Dho 794, an H6 chondrite. Mössbauer spectra and XRD patterns of dated ordinary chondrites from the Daraj locality of the Libyan Sahara, the Nullarbor region of Australia, and Roosevelt County, New Mexico, USA, suggest a suite of ferric iron weathering products that include goethite, magnetite, maghemite, ferrihydrite, lepidocrocite, and akaganéite (Bland et al. 1996).

In contrast to Fe-Ni, troilite undergoes gradational changes during alteration with diffuse boundaries between fresh and altered phases, commencing with a decreased reflectivity associated with a development of microfractures on {0001}. An undetermined sulfidic alteration phase is being developed at this stage. Strongly anisotropic marcasite is found in some samples, and a thin film of pyrite precipitated at the contact between troilite and Fe oxides and hydroxides. If oxidation of all sulfides is completed, hydroxides are the major product of troilite weathering with only minor maghemite and hematite present, magnetite was not observed.

Calcite is commonly found as fine-grained, filling in

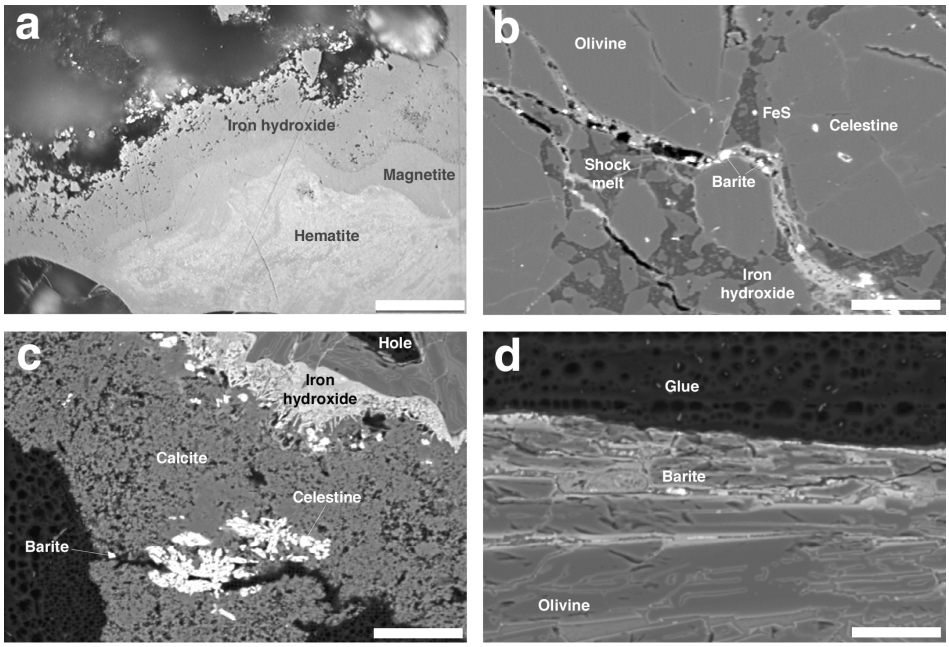

Fig. 3. Alteration mineralogy: a) reflected light micrograph illustrating different layers of weathering products of metal and troilite in Al Huqf (AH) 010. Scale bar is 20 µm. b) Network of fissures in Dho 813 filled with iron hydroxides, barite and celestine. Scale bar is 40 µm. c) Large crack in Dho 835 filled with Sr-bearing calcite (<1 wt% SrO), in which idiomorphic crystals of celestine and isolated barite occur. Iron hydroxide rims the fusion crust visible on the top right of image. Scale bar is 25 µm. d) Partially crystallized fusion crust in Dho 835 showing weathering on its outer side (top). The lighter-colored material on top is glassy material altering to hydroxides. These areas are also chlorine-enriched. Scale bar is 50 µm. Figs. 3b, 3c, and 3d are BSE images.

fractures associated with metal alteration products, and also occurs as a surface coating on those parts of meteorites originally buried in the soil. Calcite also occurs in minor amounts occluding intergranular pores in weathered meteorites. Calcite is precipitated as crystals with a maximum size of 20–30 µm sized crystals from water during occasional wetting of the meteorites (rainwater, temporary ponds, and dew) and may enclose sand grains or silt from the surrounding soil. Microcrystalline quartz of clearly secondary origin is occasionally observed in small pores in the matrix, typically within secondary Fe hydroxides.

In three ordinary chondrites with high Ba and Sr concentrations (Dho 813, Dho 835, and Shişr 020; Table 1), tiny barite and celestine crystals (Figs. 3b, 3c, and 3d) with a maximum grain size of 10 µm were detected. The crystals occur mainly in fractures and in voids filled with iron oxides/hydroxides, calcite, or anhydrite. In Fig. 3c, two clusters of celestine grains occur associated with Sr-bearing calcite (<1 wt% SrO), in sample Dho 835 barite crystals occur aligned in a chlorine-enriched alteration product replacing fusion crust glass (Fig. 3d). As well as barite and celestine, Ba-rich celestine grains were also observed.

A pale green mineral, which is confined to the lower part of meteorite surfaces (in direct contact with soil) and within fractures of weathered ordinary chondrites, is frequently observed. This material usually occurs as a thin layer without visible crystals and occasionally can be observed on soil particles in direct contact with meteorites.

For identification of the green material, three samples were analyzed (two from JaH 073 and one from JaH 070) using X-ray diffraction (XRD) on a Si single crystal plate. To obtain compositional information, some analyses of the green material from a third sample from the meteorite JaH 073 were performed by EDS. Since the samples originate from the lower part of the meteorite fixed in the soil, they are contaminated with soil minerals such as quartz, calcite, and sometimes dolomite. Results from chemical analysis of the green material match characteristics of the serpentine group minerals nepouite and pecoraite ($Ni_3Si_2O_5(OH)_4$), the Ni-analogs of lizardite (nepouite) and clinochrysotile (pecoraite). Pecoraite is a known weathering product of iron meteorites in desert environments (Faust et al. 1969; Lee and Bland 2004). XRD patterns show three relatively broad reflections at 7.5, 3.8, and 2.5 Å, indicating poorly crystallized material. The EDS analyses correspond to a Ni/Si atomic ratio of 3.6:2. We tentatively identify this mineral as Ni-serpentine. The Ni/Co ratio ranges between 14 and 44 with an average of 29 (chondritic ratio is 20) for 5 analyses, indicating a preferential enrichment of Ni in serpentine minerals during weathering.

Chemistry of Meteorite Alteration

The geochemical analysis of the ordinary chondrite finds investigated and their comparison to mean unweathered H and L chondrite compositions (Mason 1971; Kallemeyn et al. 1989; Hofmann et al. 2000; Friedrich et al. 2003) demonstrate

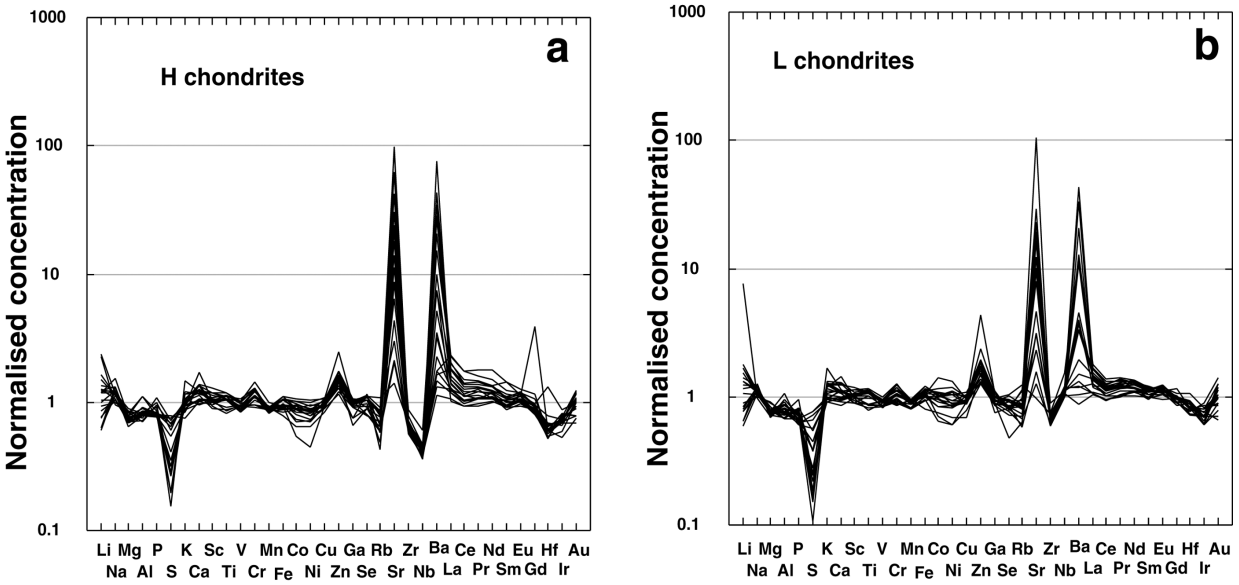

Fig. 4. Logarithmic plots of the bulk chemical composition of weathered H chondrites (a) and (b) L chondrite finds normalized to the mean bulk chemical composition of unweathered H and L chondrites (Mason 1967). Sr and Ba are strongly enriched relative to the mean chondritic abundance; smaller enrichments are observed for Li and Zn. Note the weak enrichment of light rare earth elements (LREE) and the depletion of S relative to the mean chondritic abundance.

that Ba and Sr concentrations in meteorites from Oman are sensitive weathering proxies that can best be correlated with the weathering grade. The less altered meteorites have relatively low concentrations of Ba and Sr (4 and 10.2 ppm, respectively), whereas heavily weathered, older meteorites contain up to 265 ppm Ba (76× chondritic) and 1140 ppm Sr (106× chondritic, Fig. 4). The L chondrites are less enriched in Ba (maximum 42× chondritic). Less altered meteorites contain up to 1.67 wt% S, while the S content decreases to 0.33 wt% in strongly altered meteorites (Table 1). Also, small enrichments of Zn and possibly Li are observed (<10× chondritic) and slight enrichments of light REE are indicated by the data (Figs. 4 and 5). Some strongly weathered meteorites are depleted in Ni (down to 0.45× chondritic). A comparison of the mean chemical composition of three terrestrial age groups (<15 kyr, 15–30 kyr, and >30 kyr) of the analyzed chondrites (Fig. 5 and Table 3) illustrates the above mentioned chemical observations as a function of terrestrial age. Loss of Mg is indicated by a lowering of the Mg/Mn ratio by 8% (L) to 10% (H) for the age group >30 kyr, as observed by Bland et al. (1998c).

The water content bound in secondary minerals of the investigated meteorites ranges from 0.72–3.37 wt% in H chondrites and from 0.1 wt% to 2.73 wt% in L chondrites (Table 1). The lowest water content in the H group was recorded for SaU 228 (W2), which yielded a terrestrial age of 9.7 ± 1.3 kyr and the highest water content was determined in JaH 102 (W4) dated at 41.4 ± 3.9 kyr. The almost unaltered Ghubara L5 chondrite (weak alteration is observed in near surface metal) has the lowest water content in the L group, the highest content was measured in the strongly altered RaS 110 (W4) dated at 23.3 ± 1.3 kyr. The water content in both H and L chondrites shows a frequency maximum at 2–2.5 wt%. It was observed that some heavily weathered younger meteorites (e.g., Uruq al Hadd [UaH] 002: 9.7 kyr; Dho 1005: 12.6 kyr; Al Huqf [AH] 011: 3.0 kyr) have water contents comparable to older falls (Table 1). The average water content for H chondrite age groups (<15 kyr, 15–30 kyr, and >30 kyr) is 1.97 wt%, 2.40 wt%, and 3.04 wt%. The average water content for L chondrites (<15 kyr, 15–30 kyr, and >30 kyr) is 1.35 wt%, 2.18 wt%, and 2.32 wt%.

A plot of water content versus terrestrial age of meteorites (Fig. 6) shows a rapid initial increase from 0–15 kyr followed by slower increase of water content for H chondrites. L chondrites also show a rapid initial increase in water content from 0–20 kyr, but older samples show no further increase with increasing age. Three H5 and three L6 chondrites from Açfer region, Algeria (Stelzner et al. 1999) show a similar curve of increasing water content with increasing age and weathering grade.

Correlation of Weathering Parameters with ^{14}C Age

In Table 1, physical, mineralogical, and chemical properties that may vary with terrestrial age are presented for 39 samples/falls for which both ^{14}C terrestrial ages and chemical analysis are available. By comparing mean values for the age groups 0–15, 15–30, and >30 kyr, the following age-dependences can be recognized: i) strongly age-dependent: Sr, Ba, S, and H_2O contents, meteorite powder

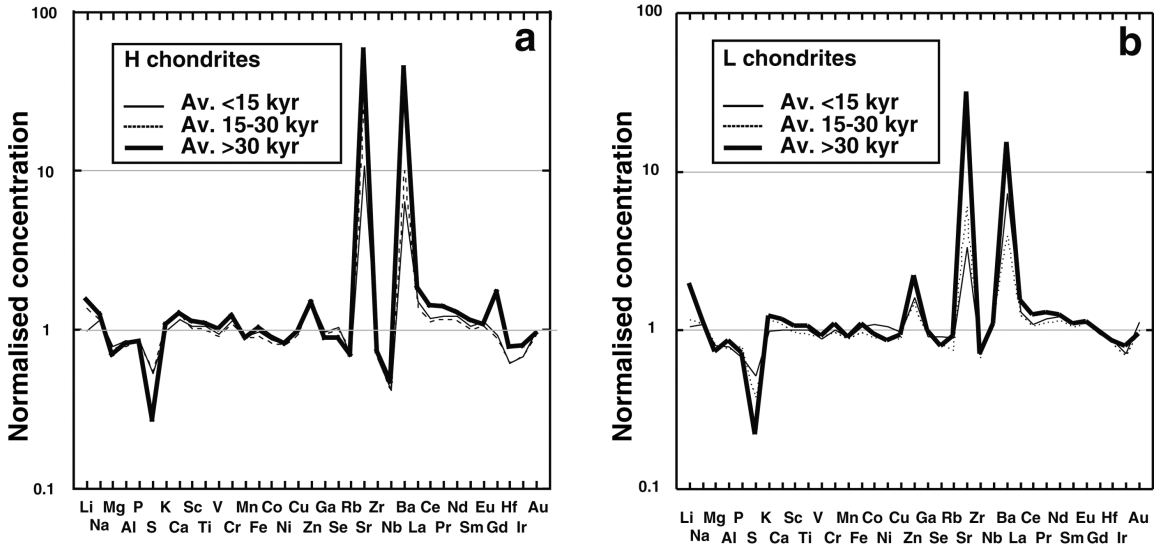

Fig. 5. Logarithmic plots of the bulk chemical composition of weathered H and L chondrites normalized to the mean chemical composition of unweathered H (a) and L chondrites (b) (Mason 1967). Data from the weathered finds are grouped into three categories <15 kyr, 15–30 kyr, and >30 kyr. Sr and Ba contents increase and S decreases with increasing terrestrial age. Small enrichments are observed for Li and Zn.

color, and width of oxide veins; ii) medium age-dependent: weathering grade, metal oxidation, troilite oxidation, fragmentation index, dispersion index, and Li; iii) weakly age-dependent: Ni, Zn, and As; iv) no clear age dependence: Fe and Co. A matrix of the correlation coefficients between the different weathering proxies and ^{14}C terrestrial ages (Table 4) at 95% confidence level supports the observations listed in Table 1. Significant positive correlations agree with properties increasing with terrestrial age. On the other hand, significant negative correlations are shown by properties declining with terrestrial age. The best correlations between different weathering proxies are observed for alteration-metal oxidation, Ba-Sr, and metal oxidation-troilite oxidation. It must be noted that there likely are relationships between terrestrial age and some of the weathering proxies that have correlation coefficients below statistical significance, e.g., oxide vein thickness. Age groups 0–15, 15–30, and >30 kyr (Table 1) show a steady increase of vein thickness with age but low correlation coefficients are due to a few strongly deviating measurements. The statistically significant decrease of Ni/Fe (Table 4) with age is supported by the observed mobility of Ni from some meteorites into the underlying soil (see below).

Soil Chemistry: Aqua Regia Extraction-OES

Analyses of 46 RSS (<0.15 mm) by aqua regia extraction-OES (Table 5) show that the surface soils are compositionally homogeneous over wide areas of the Oman interior desert, even though the areas are underlain by different marine and lacustrine stratigraphic units (Fig. 7a). This indicates strong aeolian mixing of surface soils over the entire desert. Compared with RSS (averaging 40 ppm Ni and 4.8 ppm Co), SUM shows significant enrichments in Ni (average 77 ppm) and Co (5.3 ppm), excluding one extreme sample containing 6752 ppm Ni and 216 ppm Co.

Compared with the average upper crustal value of 20 ppm Ni and 10 ppm Co (Taylor and McLennan 1985), SUM are enriched in Ni, whereas Co is enriched only in a few samples where the Ni content exceeds 240 ppm (Fig. 8b). In the most extreme case, SUM show a Ni value which is 337 times the average crustal content and a Co value of 21.5 times crustal (Fig. 8b). RSS show a weak enrichment of Ni (up to 47 ppm), but no clear enrichment of Co is observed (Figs. 7a and 8a). Also, S and Ca in SUM and RSS are enriched relative to average crustal values. While the sulfur enrichment can be explained by the presence of gypsum in the desert soil and Ca is derived from limestone, the reason for the Ni enrichment is not obvious. Two calcretes sampled at 20 cm below the surface show high Sr concentrations of 1370 and 2900 ppm (average 2133 ppm Table 5), indicating a significant mobility of Sr during recent soil formation processes.

Differences in composition between RSS and SUM samples are evidently a result of the mobilization of Ni and Co from the overlaying meteorite to the underling soil during chemical weathering. Ni tends to leach from limonite as a result of weathering of Fe-Ni metal in ordinary chondrites (Norton 2002). In cases where the SUM Ni and Co concentrations were higher than in the reference sample (RSS), the Ni/Co ratio of the contamination $(Ni/Co)_{met}$ was calculated as follows: $(Ni/Co)_{met} = Ni\ (SUM) - Ni\ (RSS) / Co\ (SUM) - Co\ (RSS)$. The $(Ni/Co)_{met}$ ratios range from 24.5 to 75 (mean 40), clearly higher than the chondritic value of 20, indicating preferential loss of Ni over Co.

Table 3. Averaged geochemical analyses of H and L chondrite age groups.

Elements	Unit	Method	Av. chondrites	<15 kyr	<15 kyr	15–30 kyr	15–30 kyr	>30 kyr	>30 kyr
H chondrites				Av. (n = 8) ± 1σ	Av./av. chondritic	Av. (n = 7) ± 1σ	Av./av. chondritic	Av. (n = 5) ± 1σ	Av./av. chondritic
Li	ppm	2	1.7	1.62 ± 0.47	0.95	2.28 ± 0.87	1.34	2.28 ± 1.09	1.34
Na	%	1	0.57	0.64 ± 0.05	1.12	0.68 ± 0.12	1.19	0.70 ± 0.04	1.23
Mg	%	3	14.2	11.11 ± 0.80	0.78	10.9 ± 0.1	0.77	10.1 ± 1.0	0.71
Al	%	3	1.01	0.85 ± 0.12	0.84	0.81 ± 0.05	0.80	0.88 ± 0.15	0.87
P	%	3	0.097	0.08 ± 0.01	0.85	0.08 ± 0.01	0.85	0.08 ± 0.01	0.85
S	%	3	2	1.15 ± 0.44	0.57	1.00 ± 0.51	0.50	0.59 ± 0.15	0.30
K	%	3	0.08	0.08 ± 0.01	0.97	0.09 ± 0.02	1.06	0.09 ± 0.01	1.03
Ca	%	3	1.2	1.36 ± 0.19	1.13	1.52 ± 0.27	1.27	1.47 ± 0.13	1.22
Sc	ppm	1	8	8.20 ± 0.63	1.03	8.44 ± 0.97	1.06	8.88 ± 0.60	1.11
Ti	%	3	0.06	0.06 ± 0.01	1.02	0.06 ± 0.01	1.03	0.07 ± 0.01	1.09
V	ppm	2	61	56.4 ± 4.1	0.92	56.3 ± 3.1	0.92	59.6 ± 3.8	0.98
Cr	ppm	1	3400	3740 ± 401	1.10	3873 ± 622	1.14	4146 ± 283	1.22
Mn	ppm	3	2260	2008 ± 54	0.89	2015 ± 132	0.89	2001 ± 89	0.89
Fe	%	1	27.6	26.6 ± 2.2	0.97	25.2 ± 2.0	0.91	28.7 ± 2.3	1.04
Co	ppm	1	834	753 ± 101	0.90	657 ± 121	0.79	770 ± 63	0.92
Ni	ppm	1	16850	14525 ± 1738	0.86	12517 ± 2597	0.74	14520 ± 1813	0.86
Cu	ppm	2	90	88.8 ± 5.7	0.99	83.7 ± 4.6	0.93	88.8 ± 7.1	0.99
Zn	ppm	3	51	75.5 ± 8.1	1.51	74.4 ± 11.0	1.49	83.7 ± 23.7	1.67
Ga	ppm	2	5.2	5.07 ± 0.53	0.98	4.93 ± 0.47	0.95	4.67 ± 0.75	0.90
Se	ppm	2	7	7.24 ± 0.79	1.03	7.06 ± 0.80	1.01	6.54 ± 0.91	0.93
Rb	ppm	2	3	2.03 ± 0.62	0.68	2.26 ± 0.36	0.75	2.21 ± 0.46	0.74
Sr	ppm	2	9.5	93 ± 104	9.79	244 ± 290	25.7	438 ± 349	46.1
Zr	ppm	2	9.5	6.23 ± 0.65	0.66	6.31 ± 0.37	0.66	6.60 ± 1.02	0.69
Nb	ppm	2	1.1	0.45 ± 0.05	0.41	0.46 ± 0.03	0.42	0.51 ± 0.09	0.46
Ba	ppm	3	3.5	20.5 ± 26.5	5.87	35.1 ± 39.5	10.0	123 ± 95	35.2
La	ppm	2	0.3	0.46 ± 0.14	1.52	0.41 ± 0.08	1.38	0.55 ± 0.10	1.82
Ce	ppm	2	0.84	1.00 ± 0.23	1.19	0.95 ± 0.13	1.13	1.18 ± 0.20	1.41
Pr	ppm	2	0.12	0.15 ± 0.03	1.22	0.14 ± 0.02	1.16	0.17 ± 0.02	1.39
Nd	ppm	2	0.58	0.71 ± 0.15	1.22	0.66 ± 0.06	1.15	0.75 ± 0.10	1.29
Sm	ppm	2	0.21	0.22 ± 0.04	1.06	0.21 ± 0.02	0.99	0.24 ± 0.04	1.14
Eu	ppm	2	0.07	0.08 ± 0.01	1.11	0.07 ± 0.01	1.07	0.08 ± 0.01	1.08
Gd	ppm	2	0.32	0.29 ± 0.04	0.92	0.29 ± 0.02	0.89	0.49 ± 0.42	1.55
Hf	ppm	2	0.25	0.15 ± 0.02	0.62	0.15 ± 0.01	0.62	0.18 ± 0.08	0.73
Ir	ppb	1	770	553 ± 41.3	0.70	517 ± 50	0.65	612 ± 45	0.77
Au	ppb	1	230	235 ± 23.1	1.02	211 ± 43	0.92	229 ± 48	0.99
L chondrites				n* = 6		n* = 10		n* = 10	
Li	ppm	2	1.8	1.91 ± 0.80	1.06	2.09 ± 0.81	1.16	3.54 ± 4.6	1.97
Na	%	1	0.65	0.72 ± 0.05	1.1	0.71 ± 0.04	1.1	0.74 ± 0.06	1.14
Mg	%	3	15.2	12.1 ± 0.9	0.8	12.1 ± 0.9	0.8	11.1 ± 0.5	0.73
Al	%	3	1.1	0.87 ± 0.10	0.79	0.84 ± 0.06	0.76	0.95 ± 0.14	0.86
P	%	3	0.11	0.07 ± 0.01	0.67	0.09 ± 0.01	0.79	0.08 ± 0.01	0.72

Table 3. *Continued.* Averaged geochemical analyses of H and L chondrite age groups.

Elements	Unit	Method	Av. chondrites	<15 kyr	<15 kyr	15–30 kyr	15–30 kyr	>30 kyr	>30 kyr
S	%	3	2.17	1.13 ± 0.53	0.52	0.81 ± 0.40	0.38	0.47 ± 0.25	0.22
K	%	3	0.09	0.09 ± 0.01	0.99	0.10 ± 0.02	1.17	0.11 ± 0.01	1.23
Ca	%	3	1.28	1.29 ± 0.09	1.01	1.40 ± 0.26	1.09	1.48 ± 0.13	1.16
Sc	ppm	1	8.9	8.97 ± 0.40	1.01	8.72 ± 0.80	0.98	9.36 ± 0.86	1.05
Ti	%	3	0.07	0.07 ± 0.01	1.01	0.06 ± 0.01	0.94	0.07 ± 0.01	1.06
V	ppm	2	65	57.8 ± 2.3	0.89	59.2 ± 2.9	0.91	59.9 ± 3.5	0.92
Cr	ppm	1	3800	3838 ± 402	1.01	3675 ± 483	0.97	4193 ± 436	1.1
Mn	ppm	3	2460	2212 ± 105	0.9	2173 ± 148	0.88	2203 ± 144	0.9
Fe	%	1	21.8	23.2 ± 1.5	1.06	21.1 ±2.3	0.97	24.1 ± 2.0	1.1
Co	ppm	1	550	599 ± 90	1.09	495 ± 60	0.9	517 ± 109	0.94
Ni	ppm	1	11530	12084 ± 1799	1.05	10215 ± 1657	0.89	9828 ± 2321	0.85
Cu	ppm	2	86	83.9 ± 5.74	0.98	77 ± 10	0.89	80.1 ± 6.9	0.93
Zn	ppm	3	50	80.3 ± 6.2	1.61	75.2 ± 8.8	1.5	110 ± 50	2.2
Ga	ppm	2	5.2	4.75 ± 0.49	0.91	4.86 ± 0.34	0.93	5.13 ± 0.51	0.99
Se	ppm	2	8.9	8.21 ± 0.83	0.92	7.32 ± 1.59	0.82	7.05 ± 0.38	0.79
Rb	ppm	2	2.8	2.51 ± 0.50	0.9	2.1 ± 0.4	0.75	2.54 ± 0.54	0.91
Sr	ppm	2	10.8	36.2 ± 18.8	3.35	64.9 ± 50	6.01	343 ± 356	31.8
Zr	ppm	2	8.9	6.25 ± 0.25	0.7	5.99 ± 0.52	0.67	6.23 ± 0.84	0.7
Nb	ppm	2	0.4	0.45 ± 0.02	1.13	0.47 ± 0.07	1.18	0.44 ± 0.03	1.1
Ba	ppm	3	3.5	25.4 ± 44.3	7.26	13.7 ± 15.2	3.92	53.2 ± 47.5	15.2
La	ppm	2	0.3	0.39 ± 0.05	1.3	0.38 ± 0.06	1.25	0.46 ± 0.06	1.53
Ce	ppm	2	0.84	0.92 ± 0.08	1.09	0.91 ± 0.10	1.08	1.04 ± 0.1	1.24
Pr	ppm	2	0.12	0.14 ± 0.01	1.18	0.14 ± 0.02	1.13	0.15 ± 0.01	1.28
Nd	ppm	2	0.58	0.71 ± 0.05	1.23	0.67 ± 0.06	1.15	0.72 ± 0.05	1.25
Sm	ppm	2	0.21	0.23 ± 0.01	1.1	0.22 ± 0.02	1.05	0.23 ± 0.02	1.1
Eu	ppm	2	0.07	0.08 ± 0.01	1.11	0.08 ± 0.01	1.12	0.08 ± 0.01	1.13
Gd	ppm	2	0.32	0.3 ± 0.01	0.94	0.31 ± 0.03	0.98	0.31 ± 0.02	0.97
Hf	ppm	2	0.18	0.16 ± 0.01	0.87	0.15 ± 0.02	0.83	0.16 ± 0.02	0.86
Ir	ppb	1	565	400 ± 46	0.71	391 ± 26	0.69	446 ± 38	0.79
Au	ppb	1	160	178 ± 23	1.12	159 ± 20	1	153 ± 41	0.95

1 = INAA.
2 = ICP-MS.
3 = ICP-OES.
Average H, L chondrite values from Mason (1971).
Average for Zn and Ir from mean of Friedrich (2003) and Kallemeyn (1989).
n* = Number of analyzed meteorites, including paired samples from strewn field.
Av. = Average.

Soil Chemistry: Total Analysis

Not surprisingly, total soil analyses (<0.15 mm) generally show higher concentrations for most elements than the aqua regia leach (Table 6). This is most evident for Cr where the leach average is 33 ppm and the total average 1427 ppm, compared with 35 ppm in mean upper continental crust (Taylor and McLennan 1985). Most elements are present at least partly in a form inaccessible to the aqua regia attack employed. Total analyses also demonstrate the homogeneity of the chemical composition of soils over the different meteorite collection surfaces in the Oman deserts independent of the underlying geological formations.

Comparing the total analysis results with the average chemical composition of the upper continental Earth crust (Taylor and McLennan 1985) shows that the RSS and SUM samples are strongly enriched in Cr (up to 80×), moderately enriched (7× to 15×) in Se, Ni, and Ca and slightly enriched in Hf, S, Ti, Mg, and Sr (Fig. 7b). Depletions relative to average upper crust are mainly observed for Ta, P, Rb, Ga, Na, Cs, K, Fe, Sc, and Al, probably due to the carbonate-rich lithology. As in leach analyses, total analyses show that soil underneath meteorites is enriched in Ni. We found chromite to be the main carrier of anomalous Cr in the soils. To test for a possible meteoritic origin, as observed in Ordovician limestones in southern Sweden (Schmitz et al. 2001, 2003), 43 chromite grains from 8 samples were analyzed with the electron microprobe (Table 7). By comparison with chondritic chromites of Schmitz et al. (2003), our ZnO, TiO_2, and Cr_2O_3 values are lower, and the Al_2O_3 and MgO values are higher than in ordinary chondrites demonstrating that the chromites are non-meteoritic in origin.

DISCUSSION

Terrestrial Ages of Omani Meteorites

The distribution of terrestrial ages of the ordinary chondrites studied (Fig. 9) shows the largest peak in the 10–15 kyr range. Only 16% of meteorites have terrestrial ages <10 kyr and 28% have ages >30 kyr, a distribution that is significantly different from other sites investigated (Sahara, Australia, western United States; Table 8) where 44–85% of samples are <10 kyr and only 0–18.5% are >30 kyr (Jull et al. 1990; Jull 1993; Bland et al. 1998c; Bland and Bevan 2000; Welten et al. 2004). The distribution of ages from Oman is more comparable with age distributions of ordinary chondrites from Roosevelt County, New Mexico, USA (Bland et al. 1998c), and the Allan Hills icefield, Victoria Land, Antarctica (Jull et al. 1998) (Table 8). Our age distribution data are very similar to those obtained on other samples from Oman and Saudi Arabia (Jull 2001).

In order to check how representative our suite of samples selected for terrestrial age dating is, we compared the weathering degrees of this suite with the weathering degree of all our finds and all published finds from Oman (Table 9). Because we intentionally included samples of low degree of weathering, these are overrepresented. The high average age of dated meteorites is consistent with the presence of a high percentage of strongly weathered (W3–4) finds.

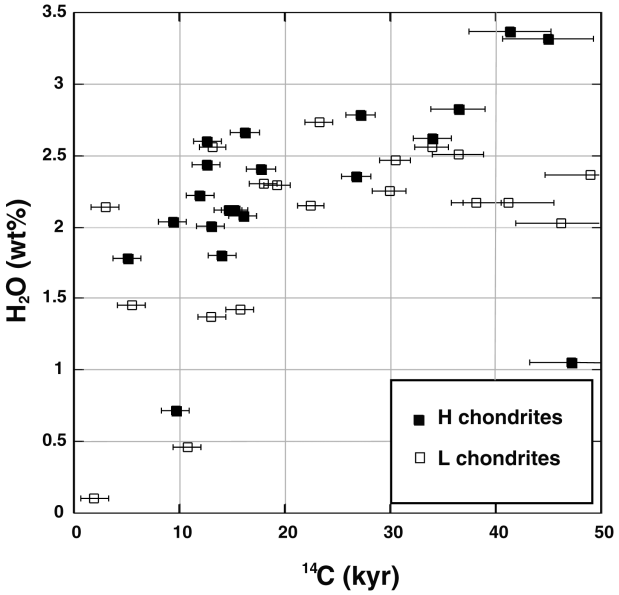

Fig. 6. Plot of water content of Omani H and L chondrites against their terrestrial age. H chondrites show an initially rapid increase of water content with age, up to ~10 kyr, followed by a period of slower increase with age. L chondrites also show an initially rapid increase in water content up to a saturation at ~20 kyr followed by a constant level with increasing terrestrial age.

The weathering rate at different sites appears to depend on local conditions, as was also observed in other hot desert regions (Bland et al. 1996, 1998c; Jull et al. 1998; Bland and Bevan 2000; Jull 2001). There may be several reasons for the relatively high average terrestrial age of Omani meteorites. Besides the unlikely possibility of sampling bias towards high terrestrial ages, it appears that the meteorite accumulation surfaces in Oman are very stable, which is supported by the find of lunar meteorite Dho 025 with a terrestrial age of 500–600 kyr (Nishiizumi and Caffee 2001). The presence of such stable and old surfaces leads to the accumulation of a high percentage of older meteorites relative to younger ones. In general, the ^{14}C terrestrial ages correlate well with the visual weathering grade and most weathering parameters (Table 1). Only a few samples differ from the general trend. Possible problems include the presence of unrecognized strewn fields (resulting in occurrence of fragments with variable and in part significant shielding to cosmic rays) and the possible contamination with terrestrial ^{14}C (that may be enclosed in inert alteration products such as quartz and magnetite). Such contamination might be an explanation for the relatively common occurrence of ages in

Table 4. Correlation matrix of weathering proxies and ^{14}C terrestrial ages at 95% confidence level.

	Age (kyr)	Weathering grade	FI	FD	Powder color	Iron oxidation (vol%)	Troilite oxidation (vol%)	Oxide veins (cm)	Ba (ppm)	Sr (ppm)	S (wt%)	Ni/Co	Ni/Fe
Age													
Weathering grade	0.64[a]												
FI	–0.23	–0.40[a]											
FD	0.09	0.16	–0.66[a]										
Powder color	0.61[a]	0.57[a]	–0.15	–0.02									
Iron oxidation	0.52[a]	0.86[a]	–0.34[a]	0.20	0.39[a]								
Troilite oxidation	0.42[a]	0.75[a]	–0.33[a]	0.11	0.48[a]	0.62[a]							
Oxide veins	0.27	0.34[a]	–0.27	0.05	0.14	0.31	0.10						
Ba	0.52[a]	0.27	0.12	0.04	0.49[a]	0.32	0.14	0.18					
Sr	0.60[a]	0.34[a]	0.11	0.00	0.50	0.29	0.22	0.05	0.85[a]				
S	–0.57[a]	–0.53[a]	0.38[a]	–0.19	–0.65[a]	–0.27	–0.54[a]	–0.14	–0.33[a]	–0.34[a]			
Ni/Co	–0.26	–0.16	0.04	0.06	–0.26	–0.04	–0.03	–0.14	–0.36[a]	–0.45[a]	0.30		
Ni/Fe	–0.41[a]	–0.39[a]	0.20	0.01	–0.61[a]	–0.36[a]	–0.40[a]	–0.04	–0.26	–0.32[a]	0.57[a]	0.50[a]	
H_2O	0.57[a]	0.68[a]	–0.34[a]	0.20	0.61[a]	0.73[a]	0.44[a]	0.39[a]	0.49[a]	0.39[a]	–0.26	–0.17	–0.28

[a]Significant values based on 95% confidence limits.

FI = Fragmentaion index.

FD = Fragment dispersion.

Table 5. Averaged leachate analyses for different soil types, Omani interior deserts.

Element	Units	MUC	RSS	RSS	SUM	SUM	Calcrete*	Calcrete
			Av. (n = 46) ± 1	Av./MUC	Av. (n = 97) ± 1	Av./MUC	Av. (n = 2) ± 1	Av./MUC
Na	%	2.89	0.11 ± 0.19	0.04	0.05 ± 0.05	0.02	0.15 ± 0.17	0.05
Mg	%	1.33	1.33.1 ± 0.3	1	1.21 ± 0.25	0.91	1.48 ± 1.16	1.11
Al	%	8.04	0.49 ± 0.07	0.06	0.45 ± 0.08	0.06	0.48 ± 0.08	0.06
P	%	0.105	0.02 ± 0.01	0.15	0.01 ± 0.01	0.13	0.01 ± 0.01	0.07
S	%	0.026	0.05 ± 0.03	1.76	0.04 ± 0.06	1.67	0.45 ± 0.43	17.4
K	%	2.8	0.08 ± 0.01	0.03	0.07 ± 0.01	0.02	0.09 ± 0.02	0.03
Ca	%	3	17.9 ± 2.05	5.97	16.6 ± 1.61	5.53	20.7 ± 4.8	6.91
Sc	ppm	11	2.55 ± 0.30	0.23	2.29 ± 0.39	0.21	1.93 ± 0.24	0.18
Ti	%	0.3	0.06 ± 0.01	0.2	0.05 ± 0.01	1.77	0.04 ± 0.01	0.15
V	ppm	60	33.3 ± 4.7	0.56	28.4 ± 5.1	0.47	30.8 ± 1.0	0.51
Cr	ppm	35	35.4 ± 6.0	1.01	30.3 ± 5.6	0.86	40.6 ± 5.2	1.16
Mn	ppm	600	222 ± 37	0.37	192 ± 32	0.32	142 ± 5	0.24
Fe	%	3.5	0.92 ± 0.12	0.26	0.80 ± 0.16	0.23	0.71 ± 0.08	0.2
Co	ppm	10	4.81 ± 1.22	0.48	5.3 ± 1.9 (7.5 ± 21.5)	0.75	3.79 ± 0.07	0.38
Ni	ppm	20	39.9 ± 19.6	1.99	76.9 ± 68.5 (146 ± 686)	7.28	27.5 ± 2.0	1.37
Zn	ppm	71	7.09 ± 5.16	0.1	5.63 ± 3.65	0.08	1.43 ± 1.3	0.02
Sr	ppm	350	260 ± 66	0.74	216 ± 63	0.62	2133 ± 1075	6.09
Zr	ppm	190	23.6 ± 5.7	0.12	23.3 ± 4.9	0.12	19.5 ± 2.54	0.1
Ba	ppm	550	89.1 ± 44.6	0.16	75.1 ± 27.3	0.14	172 ± 167	0.31
La	ppm	30	8.8 ± 1.5	0.29	7.77 ± 1.41	0.26	5.86 ± 0.42	0.2
Pb	ppm	20	7.6 ± 1.6	0.38	7.09 ± 3.55	0.35	8.25 ± 1.82	0.41

Ni and Co values in parentheses are the average values, including the anomalous sample.
MUC = Mean Earth upper continental crust values, from Taylor and McLennan (1985).
n = Number of analysis.
Av. = Average.
RSS = Reference soil samples.
SUM = Soil under meteorite.
* = Calcrete samples from 20 cm below the surface.

the 35–45 kyr range, many, but not all, of which may actually be >50 kyr. Leaching experiments demonstrated that in some cases ^{14}C can be removed from the Fe-alteration phases, indicating that several dpm/kg of ^{14}C may be due to terrestrial contamination. Modern terrestrial carbon has a ^{14}C activity of 13,560 dpm/kg, 270 times more than the saturation activity in ordinary chondrites. Therefore, a contamination with only 100 ppm of modern terrestrial carbon adds 1.36 dpm/kg of ^{14}C and in this case would reduce the apparent terrestrial age from >45 to 30 kyr. In meteorites with younger terrestrial ages this effect is obviously less severe because alteration products are less abundant and low degrees of contamination have less effect on the terrestrial age (100 ppm of modern terrestrial carbon results in an age reduction from 15.0 to 13.8 kyr). In a recent study by Welten et al. (2004) on meteorites from the Dar al Gani region, Libya, a ^{14}C terrestrial age of 34.4 ± 0.9 kyr on an H4 ordinary chondrite (DaG 343) was obtained. However, both the weathering-normalized ^{36}Cl and the ^{41}Ca concentration point to a terrestrial age of ~150 kyr (with large uncertainty). This discrepancy may be due to ^{14}C contamination.

We believe that ^{14}C terrestrial ages are good approximations for residence times on Earth, but for meteorites >30 kyr they must be regarded as minimum ages because of the aforementioned possibilities of contamination. Four meteorites (8%) have no detectable ^{14}C (two of them after Fe-hydroxide leaching) giving ages of >45 kyr. Compared to other hot deserts, no meteorites with ^{14}C terrestrial age of >42 kyr are reported from the Sahara Desert, but two are reported from the western United States and two from Roosevelt County, USA (Bland et al. 1998b, 1998c; Jull et al. 1990, 1993; Welten et al. 2004). Climatic variations may also be an important factor affecting the terrestrial age distribution of meteorites. The frequency maximum of ages at 10–15 kyr corresponds to a period of dry climate similar to present-day conditions (Sanlaville 1992), which was followed by an enhanced period of monsoon activity at 9.6 kyr (Fleitmann et al. 2003). It appears possible that initial weathering under dry conditions seals pores with Fe hydroxides, slowing down further weathering and increasing the rate of survival of meteorites from certain time periods (Bland et al. 1996, 1998a). Hence, in order to understand the deficit of younger meteorites, we would have to assume that there was selective removal of younger meteorites. There is no evidence to support this observation from the available data.

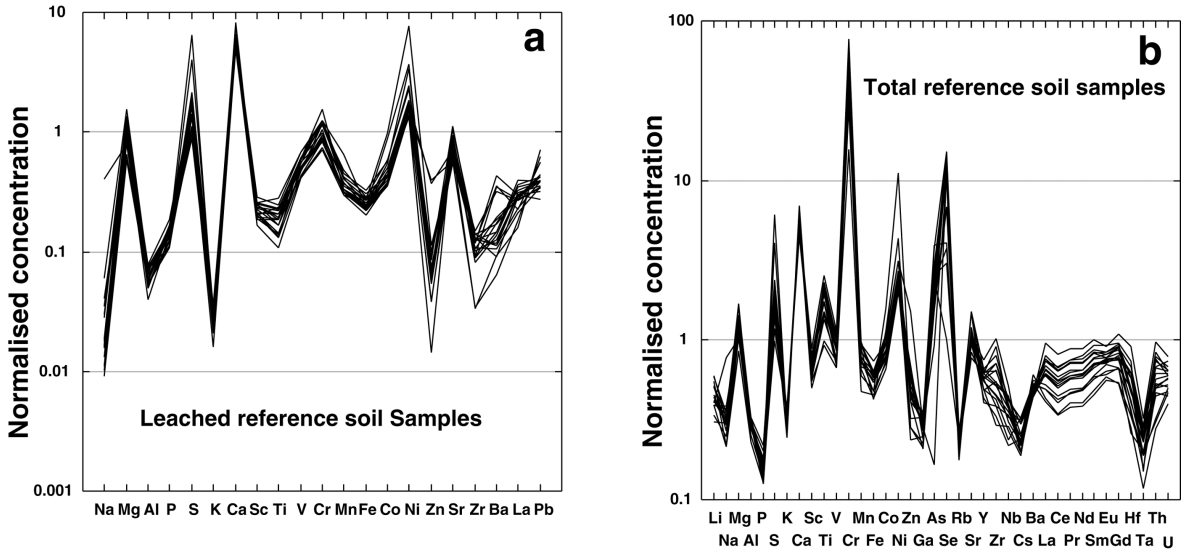

Fig. 7. a) Logarithmic plot of reference soil leachate samples normalized to mean upper continental crust values (Taylor and McLennan 1985). The reference soil samples are mainly enriched in Ca, S, and Ni, depleted in Na, K, Zn, Al, Zr, and Ba. b) Logarithmic plot of total reference soil samples normalized to mean upper continental crust values. The reference soil samples are strongly enriched in Cr, Sc, Ni, Ca, S, Ti, Mg, Sr, and depleted in Ta, P, Rb, Ga, Na, Cs, K, Fe, Sc, and Al.

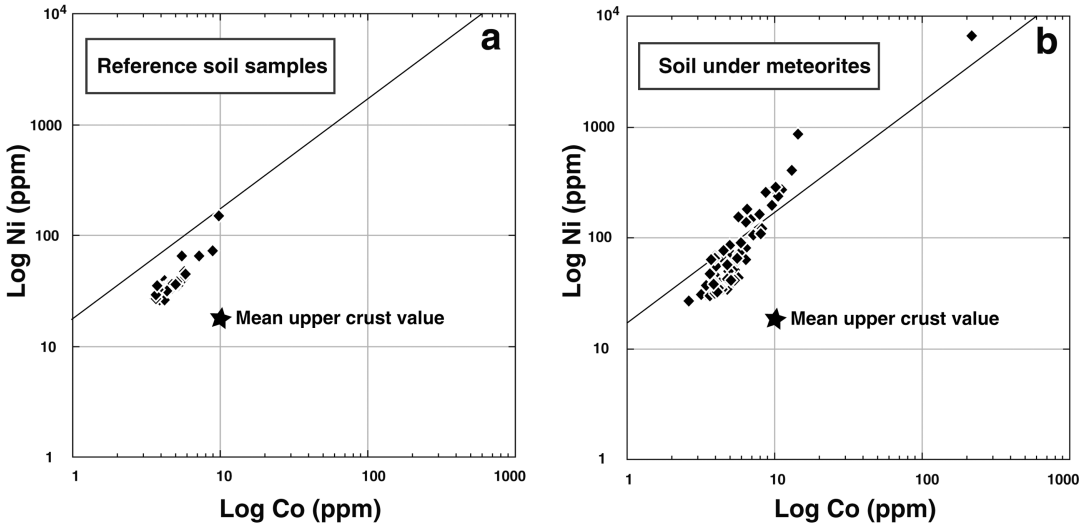

Fig. 8. Logarithmic plot of Ni versus Co content (leachates) in reference soil samples (a) and soil under meteorite samples (b) showing local strong mobilization of these elements from the meteorite to the underlying soil as a result of the weathering process. The reference line represents the chondritic Ni/Co ratio.

Weathering of Meteorites: General

It is likely that meteorites weather more intensely in wet and humid areas, and that the older meteorites are stronger weathered. Temperature fluctuations from summer to winter and between day and night could affect the weathering intensities. The alteration of meteorites starts as soon as they arrive on the Earth's surface due to chemical (water, air, salts), physical (temperature fluctuations, wind) and possibly biological (microbial activity) influences. The presence of water and oxygen will oxidize the metal, troilite, and hydrate the ferromagnesian minerals, leading to a volume increase of the meteorite. The complete transformation of 10 vol% iron metal (molar volume 7.12 cm^3), in an H chondrite to goethite (molar volume 20.76 cm^3) results in a volume increase of 19% (10% for L chondrites). Taking into account the complete transformation of 5.5 wt% troilite in H chondrites (6.0 in L chondrites), the total volume increase in H chondrites will be 19.8% (10.2% for L chondrites). The volume increase will be partially buffered by intergranular

Table 6. Averaged total analyses of soil under meteorite and reference soil samples, Omani interior deserts.

Element	Unit	Method	MUC	RSS	RSS	SUM	SUM
				Av. (n = 18)	Av./MUC	Av. (n = 12)	Av./MUC
Li	ppm	2	20	8.9 ± 1.7	0.45	8.05 ± 0.91	0.4
Na	%	1	2.89	0.97 ± 0.35	0.34	0.96 ± 0.15	0.33
Mg	%	3	1.33	1.64 ± 0.29	1.24	1.4 ± 0.26	1.06
Al	%	3	8.04	2.39 ± 0.21	0.3	2.45 ± 0.30	0.3
P	%	3	0.11	0.02 ± 0.01	0.16	0.02 ± 0.01	0.14
S	%	3	0.026	0.05 ± 0.03	2.04	0.08 ± 0.14	3.04
K	%	3	2.8	0.92 ± 0.1	0.33	1.03 ± 0.16	0.37
Ca	%	3	3	15.9 ± 1.9	5.3	14.8 ± 2.6	4.94
Sc	ppm	1	11	7.68 ± 1.09	0.7	6.79 ± 1.28	0.62
Ti	%	3	0.3	0.53 ± 0.13	1.77	0.47 ± 0.14	1.55
V	ppm	2	60	53.1 ± 8.48	0.89	43.6 ± 11.5	0.73
Cr	ppm	1	35	1600 ± 571	45.7	1253 ± 676	36
Mn	ppm	3	600	471 ± 80	0.78	405 ± 98	0.67
Fe	%	1	3.5	1.98 ± 0.30	0.57	1.69 ± 0.38	0.48
Co	ppm	2	10	9.17 ± 2.11	0.92	9.64 ± 3.40	0.96
Ni	ppm	2	20	61.6 ± 41.2	3.08	126 ± 123	6.32
Zn	ppm	3	71	36.2 ± 19.6	0.51	33.4 ± 15.2	0.47
Ga	ppm	2	17	4.92 ± 0.78	0.29	4.79 ± 0.97	0.28
As	ppm	1	1.5	3.39 ± 1.35	2.26	2.95 ± 0.75	1.97
Se	ppm	2	0.05	0.49 ± 0.23	9.88	0.46 ± 0.23	9.21
Rb	ppm	2	112	25.1 ± 2.35	0.22	26.5 ± 2.5	0.24
Sr	ppm	2	350	381 ± 76.5	1.09	351 ± 111	1
Y	ppm	2	22	12.9 ± 1.9	0.57	11.1 ± 2.2	0.51
Zr	ppm	2	190	109 ± 38.3	0.57	98.3 ± 34.2	0.52
Nb	ppm	2	25	9.04 ± 1.94	0.36	8.13 ± 2.16	0.33
Cs	ppm	2	3.7	0.91 ± 0.17	0.25	0.84 ± 0.11	0.23
Ba	ppm	3	550	271 ± 26.2	0.49	311 ± 58.8	0.57
La	ppm	2	30	19.2 ± 4.23	0.64	16.4 ± 4.7	0.55
Ce	ppm	2	64	34.8 ± 8.0	0.54	29.3 ± 8.6	0.46
Pr	ppm	2	7.1	4.31 ± 0.95	0.61	3.68 ± 1.02	0.52
Nd	ppm	2	26	16.1 ± 3.5	0.62	13.6 ± 3.7	0.52
Sm	ppm	2	4.5	3.26 ± 0.67	0.72	2.77 ± 0.71	0.62
Eu	ppm	2	0.88	0.66 ± 0.09	0.75	0.6 ± 0.1	0.68
Gd	ppm	2	3.8	3.03 ± 0.56	0.8	2.65 ± 0.65	0.7
Hf	ppm	2	5.8	2.94 ± 0.98	0.51	2.63 ± 0.89	0.45
Ta	ppm	2	2.2	0.50 ± 0.12	0.23	0.46 ± 0.15	0.21
Th	ppm	2	10.7	6.25 ± 2.05	0.58	4.83 ± 1.9	0.45
U	ppm	2	2.8	1.62 ± 0.29	0.58	1.39 ± 0.36	0.5

1 = INAA.
2 = ICP-MS.
3 = ICP-OES.
MUC = Mean Earth upper continental crust values, from Taylor and McLennan (1985).
n = Number of analysis.
Av. = Average.
RSS = Reference soil samples.
SUM = Soil under meteorite.

porosity, demonstrated by Lee and Bland (2004). Based on a typical chondrite porosity of 10 vol% (Consolmagno et al. 1988), L chondrites with low porosity and most H chondrites will experience a significant bulk volume increase.

The volume increase results in the development of cracks and an appearance similar to bread crust (Fig. 2b). Widening of cracks may occur by daily temperature fluctuations combined with a mechanical infiltration of sand grains into cracks and eventually leads to the fragmentation of the meteorite (Fig. 2c). Recent work showed that thermal effects such as diurnal heating and cooling are very important in fracturing rocks in semi-arid landscapes (McFadden et al. 2005). Cracks are filled with iron oxides or hydroxides and calcite.

Omani meteorites are generally characterized by weathering grades ranging from W1 to W4 (Wlotzka 1993).

Table 7. Omani soil chromites compared with fossil meteorite chromites.

Chromite source	RSS	Ophiolite	Extraterrestrial
Location	Oman	Oman	South Sweden
No. of grains	43		323
SiO_2	0.13	0	n.a.
Cr_2O_3	44.01	49	57.4
Al_2O_3	23.47	19.9	5.8
MgO	12.19	15	2.5
TiO_2	0.17	0.4	2.9
V_2O_5	n.a.	n.a.	0.9
Fe_2O_3	1.55	n.a.	n.a.
FeO	16.44	14.7	27.7
MnO	0	0.43	0.81
NiO	0.1	n.a.	n.a.
ZnO	0.16	n.a.	0.82
CaO	0.07	0.02	n.a.
Total	98.29	99.45	98.9

RSS = Reference soil samples.
n.a. = Not analyzed.
Extraterrestrial chromite grains from Schmitz et al. (2003).
Ophiolitic chromites from Arai et al. (2004).

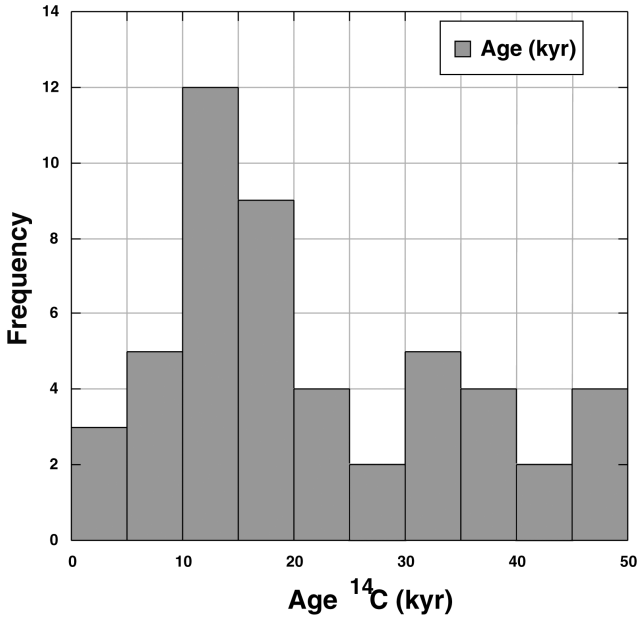

Fig. 9. Terrestrial age frequency histogram of 50 ordinary chondrites from Oman showing a peak at 10–15 kyr. The range 0–10 kyr old meteorites account for 16%, whereas 28% meteorites are older than 30 kyr. Four meteorites without detectable ^{14}C are shown in the 45–50 kyr bar.

Interestingly, only a few W5 and no W6 meteorites were identified in Oman either by us or other classification teams (Grossman 2000; Grossman and Zipfel 2001; Russell et al. 2002, 2003, 2004), which suggests a relatively high stability of olivine and pyroxene under desert conditions. Because of the lack of weathering grades >4 even in the few samples with terrestrial ages >50 kyr, the fate of highly weathered meteorites remains unclear. Fluctuations in past climatic conditions such as the peak of Indian Ocean monsoon precipitation at about 9.6 kyr (Fleitmann et al. 2003) may explain the strong weathering (W4) of some (probably paired) Dhofar meteorites (Dho 020, 787, and 1005; Table 1) that have fallen shortly before this wet period as their terrestrial ages range from 12–12.7 kyr. Similarly, it seems possible that the abundance peak of meteorites preserved at 10–15 kyr coincides with the strongly arid period between 10 and 20 kyr (e.g., Sanlaville 1992). Factors like the details of soil-meteorite relationships (local topography, depth of burial), the climatic conditions, aeolian abrasion, age of the meteorites, the composition and porosity of the meteorites are factors likely to influence weathering. It seems that under the present climatic conditions physicochemical disintegration is one of the most important weathering factors.

Weathering of Meteorites: Geochemistry

The most consistent and systematic effects of meteorite weathering seen in the geochemical data are an increase of Sr, Ba, H_2O, and depletion of S concentrations with increasing terrestrial age (Figs. 6 and 10). The clear increase of Ba and Sr concentrations with terrestrial age (Fig. 10) can be used as a proxy for terrestrial age. Dho 807 deviates from the above observed trends, as all weathering parameters point to a younger age in contrast to the obtained >47 kyr (by repeat dating using different aliquots). Enrichment and depletion effects are observed for some other elements (Li, Zn, possibly LREE) but to a much smaller degree (Fig. 4 and Fig. 5). Our observations of the enrichment of Ba, Sr, and H_2O with increasing terrestrial age of ordinary chondrites from Oman are similar to results obtained on chondrites from Açfer region, Algeria (Stelzner et al. 1999).

During weathering stages W1–W4 most of the water incorporated by meteorites is bound to iron hydroxides formed by metal oxidation. Total oxidation of 10 vol% metal in H chondrites (5 vol% in L chondrites) and of troilite (4.0 vol% in H, 4.4 vol% in L chondrites, calculated from mean S in unweathered chondrites (Mason 1967), to goethite would yield a water content of 3.64 wt% for H chondrites and 2.39 wt% for L chondrites. The maximum observed values of 3.37 wt% for H chondrites and 2.73 wt% for L chondrites are partially above calculated levels. The excess water could be within clays and phyllosilicates. A strongly weathered meteorite (W5) from the Açfer region, Algeria (Stelzner et al. 1999) has the highest water content reported for a weathered ordinary chondrite (9 wt%). This meteorite shows significant replacement of olivine and pyroxene by the phyllosilicates serpentine and/or smectite. A plot of Ba and Sr concentrations against water content (Fig. 11) shows only minor Ba and Sr enrichment up to 2 wt% water, followed by a stronger absorption trend for samples with >2 wt% water. This

Table 8. Statistics of Omani terrestrial ages compared with data from other hot deserts and Allan Hills, Antarctica (all ordinary chondrites).

Location	Reference	n	Median	Mean	St. dev.	Range	% 0–10 kyr	% >30 kyr
HaH, Libya	Jull et al. 1990	13	5.4	8.3	8.7	3.5 to 35	84.6	7.7
Nullarbor, Australia	Bland et al. 1998, 2000	36	6.4	12.2	11.7	0.7 to 33.4	58.3	11.1
Açfer, Algeria	Bland et al. 1998	51	10.3	11.6	8.6	0.67 to 42.4	49	3.9
Western USA	Jull et al. 1993	27	11.6	15.8	13.8	0 to >47.5	44.4	18.5
Dar al Gani, Libya	Welten et al. 2004	17	14.8	14.4	9.7	2.5 to >31	41.2	5.9
Oman	This study	50	17.9	21.5	13	2 to >49	16	28
Allan Hills, Antarctica	Jull et al. 1998	72	26.2	23.9	13.5	0.3 to 48	22.2	43.1
Roosevelt County, USA	Bland et al. 1998	18	26.3	27.2	11.1	7.0 to >46.0	11.1	38.9

Table 9. A comparison of weathering grades of Omani ordinary chondrites.

	Omani OC[a]	This study OC[b]	Dated samples
n	1264	263	50
	%	%	%
W0	0.4	0	2
W1	4.5	2.7	8
W2	15.9	15.6	26
W3	46.5	40.3	24
W4	32.7	41.4	40

[a]From The Meteoritical Bulletin, No. 84–88.
[b]Omani-Swiss meteorite search campaigns 2001–2003.

indicates that initially weathering is restricted to Fe-Ni metal, while troilite remains fresh to only partially weathered. Only during advanced weathering is troilite oxidized (metal is completely to strongly weathered) (Table 1 and Fig. 12) resulting in a release of sulfur which reacts with Ba and Sr derived from the soil porewater to form barite and celestine of low solubility (Figs. 3b, 3c, and 3d). This is supported by the occurrence of barite, celestine, and anhydrite crystals in fractures and holes filled by iron oxides/hydroxides and calcite. Also barite is reported from a number of weathered meteorites from Sahara (Bischoff and Geiger 1995).

Correlation of Weathering Parameters with ^{14}C Age

Norton (2000) compared weathering grades with the terrestrial ages of meteorites collected from Roosevelt County, New Mexico (Wlotzka et al. 1995), and came up with the following relationship: W2: 0.5–15 kyr; W3: 15–30 kyr; W4: 20–35 kyr; W5 and W6 30 to >45 kyr. In comparison, the meteorites from our Omani collection show a similar increase in the degree of weathering with age, but with some significant differences. We found that meteorites with weathering grades W3 and W4 have terrestrial ages of >30 kyr (Table 1). In contrast, some young meteorites (12–16 kyr) also show weathering grades of W4. One possible explanation for this behavior could be the temporary burial of the meteorite in the subsoil, where higher humidity and higher salt contents may result in a more intense alteration of metal and troilite relative to meteorites remaining on the surface. Another influence is the morphology of the surface; meteorites lying in small depressions where water ponds during heavy showers and salts accumulate after evaporation show more rapid rates of weathering. This may cause meteorites from the same fall to have variable weathering grades, as observed in the SaU 001 and JaH 073 strewn fields. Similar observations are reported from the Dar al Gani meteorite field, Libyan Sahara (Schlüter et al. 2002).

Weathering of ordinary chondrites in Oman follows two steps: a rapid initial oxidation followed by a steady rate of weathering, since most metal in the meteorites is completely altered at ~20 kyr (Fig. 13). Mössbauer determination of oxidation of H, L (LL) ordinary chondrites (Bland et al. 1996), from the Daraj locality of the Libyan Sahara; the Nullarbor region of Australia, and Roosevelt County, New Mexico, USA, show a similar rapid initial oxidation followed by a more gradual weathering. These authors proposed that a new meteorite fall arriving on Earth weathers rapidly owing to its high initial porosity. Newly formed weathering products from the oxidation of Fe-Ni metal, troilite, and ferromagnesian silicates block the pores, thus reducing the ability of water to penetrate the sample and consequently make further degradation slower. For the initial step, our results agree with this explanation, but for the second step our observations in Oman show that metal is completely altered in most meteorites with a terrestrial age ≥20 kyr. However, slow weathering will continue as a result of the alteration of troilite and ferromagnesian silicates (not observed in this study) and due to physical weathering under the influence of climate.

Soil Geochemistry and Heavy Minerals

Our data demonstrate that the chemistry of soils is very homogeneous throughout the meteorite collection areas in central Oman so that the influence of soil chemistry on meteorite weathering can be taken as constant for all meteorites recovered.

The high Cr and Ni concentrations observed in reference soils from various regions of the Oman Desert, relative to the upper continental crust, are due to the presence of detritus from the Semail ophiolite located to the northeast of the searched regions. The high Cr (Table 7) concentrations are

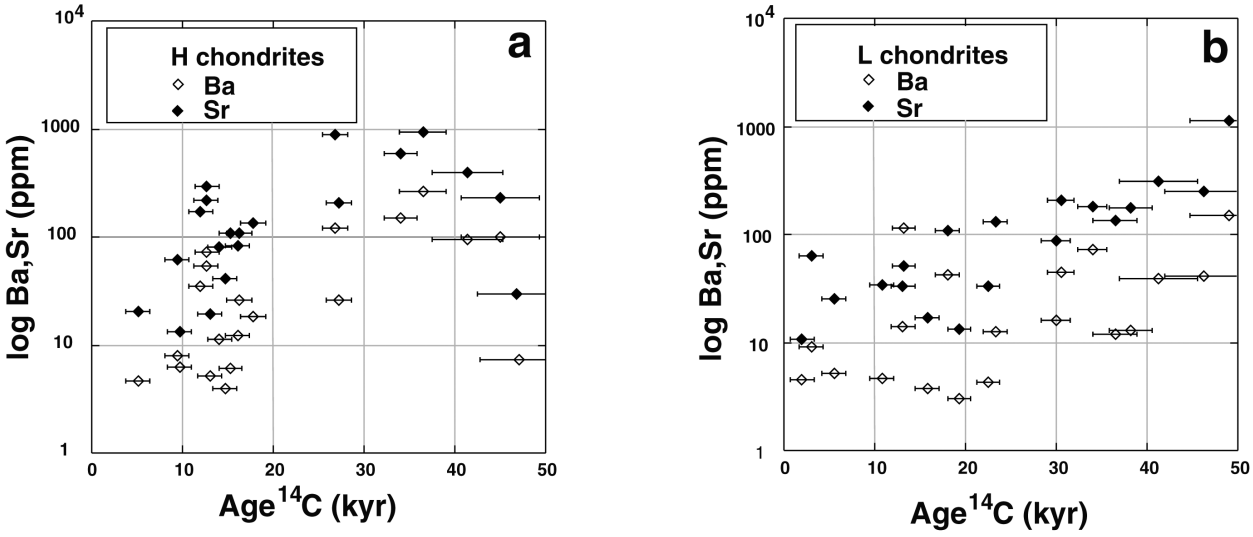

Fig. 10. a) Logarithmic plot of Ba and Sr concentrations in H (a) and L chondrites (b) versus terrestrial age indicating an increase in Ba and Sr content with increasing terrestrial age. Note that the H chondrites show a steeper slope than the L chondrites.

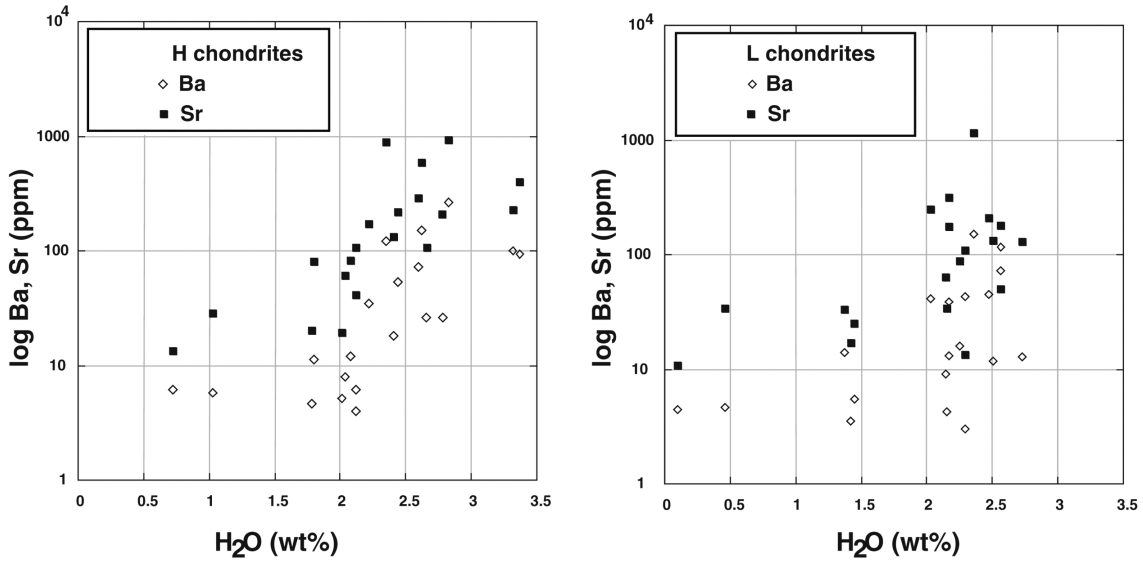

Fig. 11. Logarithmic plots of Ba and Sr versus water content in H (a) and L chondrites (b). Both H and L chondrites show an initial weak absorption of Ba and Sr followed by a steeper absorption trend beginning at ~2 wt% water. This indicates that sulfide alteration is the driving force for Ba and Sr uptake.

correlated with the presence of ophiolitic mantle chromite (Arai et al. 2004). A further argument for a detrital origin is the gradual decrease of Cr and Ni concentrations in soil with increasing distance to the alluvial fans rich in ophiolitic rocks derived from the Oman Mountains.

CONCLUSIONS

The effects of weathering on ordinary chondrites collected in the central deserts of Oman are comparable with results obtained on meteorites from other hot desert environments (Jull et al. 1993; Bland et al. 1996; Stelzner et al. 1999). Initial fast oxidation of iron metal is followed by more gradual oxidation of troilite. No weathering grades exceeding W4 were observed, indicating a considerable stability of pyroxene and olivine in this desert environment. We believe that fragmentation is a result of the combined effects of volume increase, diurnal thermal cycling, and infiltration of soil material into cracks due to wind and water. Geochemically, the major influences of weathering are an accumulation of Sr, Ba, and H_2O, and a loss of S. Soils under meteorites are contaminated with Ni and Co, Ni/Co ratios higher than chondritic values indicate a higher mobility of Ni.

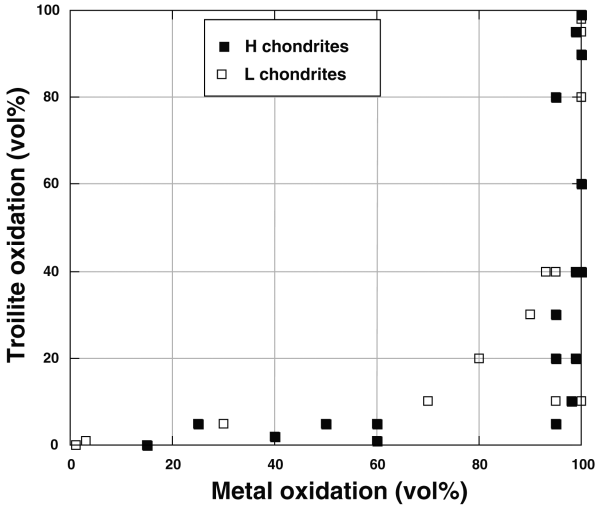

Fig. 12. Metal oxidation against troilite oxidation estimated using reflected light microscopy. The plot demonstrates that the oxidation of troilite is slower than that of metal, and troilite oxidation only goes to completeness after total oxidation of metal.

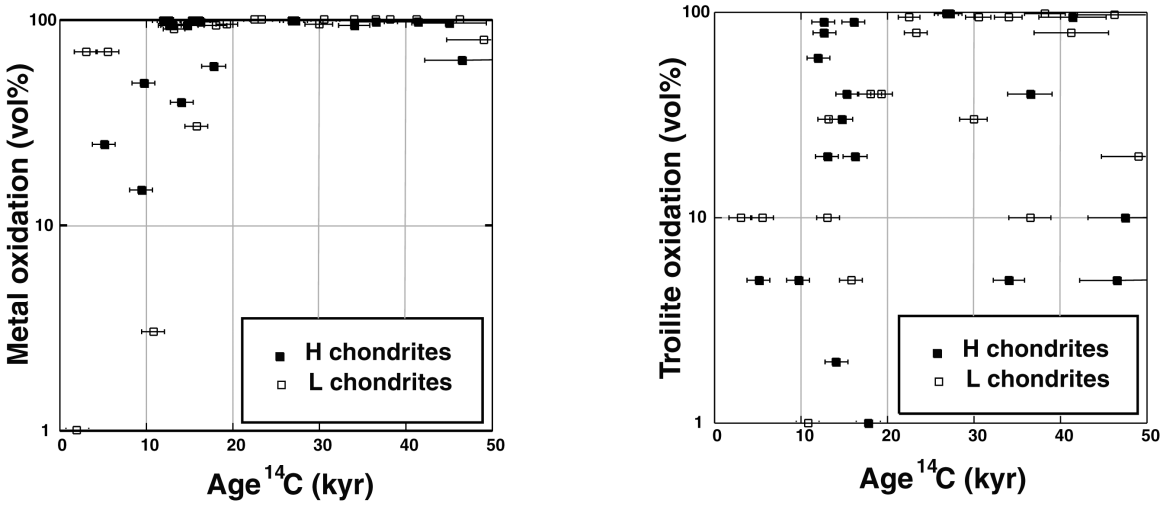

Fig. 13. a) Percentage (vol%) of metal oxidation in H and L chondrites versus terrestrial age showing complete iron metal oxidation within 20 kyr. b) percentage (vol%) of troilite oxidation in H and L chondrites versus terrestrial age. The trend is similar to the metal oxidation but the degree of oxidation is more variable and oxidation remains incomplete in many samples up to 50 kyr.

The changes observed in mineralogy and chemistry as a function of terrestrial age are consistent with a weathering process controlled by a combination of rapid iron metal oxidation and slow troilite oxidation. Fast iron metal oxidation is correlated with rapid rates of water absorption. The slower oxidation of troilite releases sulfate, allowing the steady precipitation of Ba and Sr sulfates over time. Thus, relative to water absorption, Ba and Sr uptake is initially slow. The initially rapid cementation of pores with iron hydroxides, followed by a more gradual weathering process, results in a general decrease of weathering rates over time. However, the rate of purely physical weathering will remain constant.

As soils from the interior Oman Desert are very homogeneous in bulk chemistry, the influence of soil geochemistry on meteorite weathering can therefore be assumed to be nearly constant over the whole study area. The local surface topography (hard/soft soil, depressions, and small hills) has an influence on the weathering of meteorites. This is evidenced by different degrees of weathering observed in individuals from a single meteorite fall. High Cr and Ni concentrations in soils are derived from the Semail ophiolite in the Oman Mountains.

Acknowledgments–Dr. Hilal Al Azri, Ministry of Commerce and Industry, Muscat, and Akram Al Muraza, Khalid Musallam Al Rawas, and Sami Al Zubaidi, Ministry of Commerce and Industry, Salalah, are thanked for their support during the project. Ruth Mäder, Manuel Eggimann, and Jeff

Johnson are thanked for analytical support. K. Welten, P. Bland, and M. Lee are acknowledged for their revision and important comments. This study was supported by the Swiss National Science Foundation (grant 2100-064929), the United States National Science Foundation (grant EAR01-15488) and the National Aeronautics and Space Administration (grant NAG5-11979).

Editorial Handling—Dr. Ian Franchi

REFERENCES

Arai S., Uesugi J., and Ahmed A. H. 2004. Upper crustal podiform chromitite from the northern Oman ophiolite as the stratigraphically shallowest chromite in ophiolite and its implication for Cr concentration. *Contributions to Mineralogy and Petrology* 147:145–154.

Bischoff A. and Geiger T. 1995. Meteorites from the Sahara: Find locations, shock classification, degree of weathering, and pairing. *Meteoritics* 30:113–122.

Bland P. A., Berry F. J., Smith T. B., Skinener S. J., and Pillinger C. T. 1996. The flux of meteorites to the Earth and weathering in hot desert ordinary chondrite finds. *Geochimica et Cosmochimica Acta* 60:2053–2059.

Bland P. A., Berry F. J., and Pillinger C. T. 1998a. Rapid weathering in Holbrook: An iron-57 Mössbauer spectroscopy study. *Meteoritics & Planetary Science* 33:127–129.

Bland P. A., Coway A., Smith T. B., Berry F. J., Swabey S. E. J., and Pillinger C. T. 1998b. Calculating flux from meteorite decay rates: A discussion of problems encountered in deciphering a 10^5–10^6 year integrated meteorite flux at Allan Hills and a new approach to pairing. In *Meteorites: Flux with time and impact effects,* edited by Grady M. M., Hutchinson R., McCall G. J. H., and Rothery D. A. London: The Geological Society. pp. 43–58.

Bland P. A., Sexton A. S., Jull A. J. T., Bevan A. W. R., Berry F. J., Thornley D. M., Astin T. R., Britt D. T., and Pillinger C. T. 1998c. Climate and rock weathering: A study of terrestrial age dated ordinary chondritic meteorites from hot desert regions. *Geochimica et Cosmochimica Acta* 62:3169–3184.

Bland P. A. and Bevan A. W. R. 2000. Ancient meteorite finds and the Earth's surface environment. *Quaternary Research* 53:131–142.

Burns S. J., Fleitmann D., Matter A., Neff U., and Mangini A. 2001. Speleothem evidence from Oman for continental pluvial events during interglacial periods. *Geology* 29:623–626.

Bydoun Z. R. 1966. Geology of the Arabian peninsula, eastern Aden protectorate, and part of Dhofar. USGS Professional Paper #560. pp. 1–49.

Chevrel S., Berthiaux A., Platel J. P., and Roger J. 1992. Explanatory notes to geological map of Shişr. Sheet NF 39-08, scale 1: 250,000. Muscat, Oman: Ministry of Petroleum and Minerals.

Consolmagno G. J., Britt D. T. and Stoll C. P. 1988. The porosities of ordinary chondrites: Models and interpretation. *Meteoritics & Planetary Science* 33:1221–1229.

Cornish L. and Doyle A. 1984. Use of ethanolmine thioglycollate in the conservation of pyritized fossils. *Palaeontology* 27:421–424.

Faust G. T., Fahey J. J., Mason B., and Dwornik E. J. 1969. Pecoraite, $Ni_6Si_4O_{10}(OH)_8$, nickel analog of clinochrysotile, formed in the Wolf Creek meteorite. *Science* 165:59–60.

Ferko T. E., Wang M.-S., Hillegonds D. J., Lipschutz M. E., Hutchison R., Franke L., Scherer P., Schultz L., Benoit P. H., Sears D. W. G., Singhvi A. K., and Bhandari N. 2002. The irradiation history of the Ghubara (L5) regolith breccia. *Meteoritics & Planetary Science* 37:311–327.

Fleitmann D., Burns S. J., Mudelsee M., Neff U., Kramers J., Mangini A., and Matter A. 2003. Holocene forcing of the Indian monsoon recorded in a stalagmite from southern Oman. *Science* 300:1737–1739.

Fleitmann D., Burns S. J., Neff U., Mudelsee M., Mangini A., and Matter A. 2004. Palaeoclimatic interpretations of high-resolution oxygen isotope derived from annually laminated speleothems from southern Oman. *Quaternary Science Reviews* 23:935–945.

Franchi I. A., Delisle G., Jull A. J. T., Hutchison R., and Pillinger C. T. 1995. An evaluation of the meteorite potential of the Jiddat al Harasis and the Rub al Khali regions of southern Arabia. LPI Technical Report #95-02. pp. 29–30.

Friedrich J. M., Wang M.-S., and Lipschutz M. E. 2003. Chemical studies of L chondrites. V: Compositional patterns for 49 trace elements in 14 L4–6 and 7 LL4–6 falls. *Geochimica et Cosmochimica Acta* 67:2467–2479.

Gnos E., Hofmann B., Franchi I. A., Al-Kathiri A., Hauser M., and Moser L. 2000. Sayh al Uhaymir 094: A new martian meteorite from the Oman Desert. *Meteoritics & Planetary Science* 37:835–854.

Gnos E., Hofmann B., Al-Kathiri A., Lorenzetti S., Eugster O., Whitehouse M. J., Villa I. M., Jull A. J. T., Eikenberg J., Spettel B., Krähenbühl U., Franchi I. A., and Greenwood R. C. 2004. Pinpointing the source of a lunar meteorite: Implications for the evolution of the moon. *Science* 305:657–659.

Goddard E. N., Trask P. D., De Ford R. K., Rove O. N., Singewald J. T., Jr., and Overbeck R. M. 1948. Rock-color chart. Boulder, Colorado: Geological Society of America. 11 p.

Grossman J. N. 2000. The Meteoritical Bulletin, No. 84. *Meteoritics & Planetary Science* 35:A199–A225.

Grossman J. N. and Zipfel J. 2001. The Meteoritical Bulletin, No. 85. *Meteoritics & Planetary Science* 36:A293–A322.

Hofmann B. A., Nyström J. O., and Krähenbühl U. 2000. The Ordovician chondrite from Brunflo, central Sweden III. Geochemistry of terrestrial alteration. *Lithos* 50:305–324.

Hughes-Clarke M. W. 1988. Stratigraphy and rock unit nomenclature in the oil-producing area of interior Oman. *Journal of Petroleum Geology* 11:5–60.

Jull A. J. T., Donahue D. J., and Linick T. W. 1989. Carbon-14 activities in recently fallen meteorites and Antarctic meteorites. *Geochimica et Cosmochimica Acta* 53:2095–2100.

Jull A. J. T., Wlotzka F., Palme H., and Donahue D. J. 1990. Distribution of terrestrial age and petrologic type of meteorites from western Libya. *Geochimica et Cosmochimica Acta* 54: 2895–2898.

Jull A. J. T., Donahue D. J., Cielaszyk E., and Wlotzka F. 1993. Carbon-14 terrestrial ages and weathering of 27 meteorites from the southern High Plains and adjacent areas (USA). *Meteoritics* 28:188–195.

Jull A. J. T., Cloudt S., and Cielaszyk E. 1998. ^{14}C terrestrial ages of meteorites from Victoria Land, Antarctica, and the infall rates of meteorites. In *Meteorites: Flux with time and impact effects,* edited by Grady M. M., Hutchison R., McCall G. J. H., and Rothery D. A. London: The Geological Society. pp. 75–91.

Jull A. J. T. 2001. Terrestrial ages of meteorites. In *Accretion of extraterrestrial matter throughout Earth's history,* edited by Schmitz B. and Peuker-Ehrenbrin B. New York: Kluwer Academic/Plenum Publishers. pp. 241–266.

Kallemeyn G. W., Rubin A. E., Wang D., and Wasson J. T. 1989. Ordinary chondrites: Bulk compositions, classification, lithophile-element fractionations, and composition-petrographic type relationships. *Geochimica et Cosmochimica Acta* 53:2747–2767.

Le Métour J., Michel J. C., Béchennec F., Platel J. P., and Roger J. 1995. *Geology and mineral wealth of the Sultanate of Oman*. Muscat, Oman: Ministry of Petroleum and Minerals. pp. 1–285.

Lee M. R. and Bland P. A. 2004. Mechanisms of weathering of meteorites recovered from hot and cold deserts and the formation of phyllosilicates. *Geochimica et Cosmochimica Acta* 68:893–916.

Mason B. 1967. Extraterrestrial mineralogy. *American Mineralogist* 52:307–325.

Mason B. 1971. *Handbook of elemental abundance in meteorites.* New York: Gordon and Breach. 555 p.

McFadden L. D., Eppes M. C., Gillespie A. R., and Hallet B. 2005. Physical weathering in arid landscapes due to diurnal variation in the direction of solar heating. *Geological Society of America Bulletin* 117:161–173.

Nishiizumi K. and Caffee M. W. 2001. Exposure histories of lunar meteorites Dhofar 025, 026, and Northwest Africa 482 (abstract). *Meteoritics & Planetary Science* 36:148–149.

Nishiizumi K., Okazaki R., Park J., Nagao K., Masarik J., and Finkel R. C. 2002. Exposure and terrestrial history of Dhofar 019 Martian meteorite (abstract #1366). 33rd Lunar and Planetary Science Conference. CD-ROM.

Norton O. R. 2002. *The Cambridge encyclopedia of meteorites.* Cambridge: Cambridge University Press. 354 p.

Platel J. P. and Berthiaux A. 1992a. Explanatory notes to geological map of Al ‘Ayn (Muqshin). Sheet NF 40-01, scale 1:250,000. Muscat, Oman: Ministry of Petroleum and Minerals.

Platel J. P. and Berthiaux A. 1992b. Explanatory notes to geological map of Hayma. Sheet NF 40-02, scale: 1:250,000. Muscat, Oman: Ministry of Petroleum and Minerals.

Platel J. P., Berthiaux A., Roger J. and Chevrel S. 1992. Explanatory notes to geological map of Shalim. Sheet NF 40-06. Muscat, Oman: Ministry of Petroleum and Minerals.

Russell S. S., Zipfel J., Grossman J. N., and Grady M. M. 2002. The Meteoritical Bulletin, No. 86. *Meteoritics & Planetary Science* 37:A157–A184.

Russell S. S., Zipfel J., Folco L., Jones R., Grady M. M., Zolensky M. E., McCoy T., and Grossman J. N. 2003. The Meteoritical Bulletin, No. 87. *Meteoritics & Planetary Science* 38:A189–A248.

Russell S. S., Folco L., Grady M. M., Zolensky M. E., Jones R., Righter K., Zipfel J., and Grossman J. N. 2004. The Meteoritical Bulletin, No. 88. *Meteoritics & Planetary Science* 39:A215–A272.

Sanlaville P. 1992. Changements climatiques dans la Péninsule Arabique durant le Pléistocène supérieur et l’Holocène. *Paléorient* 181:5–26.

Schlüter J., Schultz L., Thiedig B., Al-Mahdi B. O., and Abu Aghreb A. E. 2002. The Dar al Gani meteorite field (Libyan Sahara): geological setting, pairing of meteorites, and recovery density. *Meteoritics & Planetary Science* 37:1079–1093.

Schmitz B., Tassinari M. and Peuker-Ehrenbrink B. 2001. A rain of ordinary chondritic meteorites in the Early Ordovician. *Earth and Planetary Science Letters* 194:1–15.

Schmitz B., Häggström T., and Tassinari M. 2003. Sediment-dispersed extraterrestrial chromite traces a major asteroid disruption event. *Science* 300:961–964.

Stelzner T., Heide K., Bischoff A., Weber D., Scherer P., Schultz L., Happel M., Schrön W., Neupert U., Michel R., Clayton R. N., Mayeda T. K., Bonani G., Haidas I., Ivy-Ochs S., and Suter M. 1999. An interdisciplinary study of weathering effects in ordinary chondrites from the Açfer region, Algeria. *Meteoritics & Planetary Science* 34:787–794.

Taylor S. R. and McLennan S. M. 1985. *The continental crust: Its composition and evolution.* Oxford: Blackwell Scientific Publications. 328 p.

Welten K. C. 1999. Concentrations of siderophile elements in nonmagnetic fractions of Antarctic H and L chondrites: A quantitative approach on weathering effects. *Meteoritics & Planetary Science* 34:259–270.

Welten K. C., Nishiizumi K., Finkel R. C., Hillegonds D. J., Jull A. J. T., Franke L., and Schultz L. 2004. Exposure history and terrestrial ages of ordinary chondrites from the Dar al Gani region, Libya. *Meteoritics & Planetary Science* 39:481–498.

Wlotzka F. 1993. A Weathering scale for the ordinary chondrites (abstract). *Meteoritics* 28:460.

Wlotzka F., Jull A. J. T., and Donahue D. J. 1995. Carbon-14 terrestrial ages of meteorites from Açfer, Algeria. LPI Technical Report #95-02. pp. 72–73.